Title: I_h Block Reveals Separation of Timescales in Pyloric Rhythm Response to Temperature Changes in *Cancewr borealis*

Abbreviated Title: I_h block reveals dynamic Temperature Response

Kyra A Schapiro http://orcid.org/0000-0001-8308-0744
JD Rittenberg http://orcid.org/0009-0008-5742-6340
Max Kenngott http://orcid.org/0000-0002-3452-6508
Eve Marder http://orcid.org/0000-0001-9632-5448

Volen Center and Biology Department, Brandeis University, Waltham, MA 02454 USA

KAS and EM conceptualized research; KAS, JDR and MK performed the investigation; KAS and JDR performed formal analysis; KAS visualized the data and wrote the original draft of the manuscript; EM acquired funding, supervised, and reviewed/edited the manuscript.

Correspondence to: Kyra Schapiro, Biology Department and Volen Center, Brandeis University, Waltham MA 02454. Email: kyraschapiro@brandeis.edu

The authors report no conflicts of interest

Funding: T32: 5T32NS007292 (KAS)
R35: 3R35NS097343 (EM)

Keywords: crustacean, crab, STG, hyperpolarization-activated inward current, Q_{10}, phase constancy, non-monotonic dynamics

Abstract

Motor systems operate over a range of frequencies and relative timing (phase). We studied the contribution of the hyperpolarization-activated inward current (I_h) to frequency and phase in the pyloric rhythm of the stomatogastric ganglion (STG) of the crab, *Cancer borealis* as temperature was altered from 11°C to 21°C. Under control conditions, the frequency of the rhythm increased monotonically with temperature, while the phases of the pyloric dilator (PD), lateral pyloric (LP), and pyloric (PY) neurons remained constant. When we blocked I_h with cesium (Cs^+) PD offset, LP onset, and LP offset were all phase advanced in Cs^+ at 11°C, and the latter two further advanced as temperature increased. In Cs^+ the steady state increase in pyloric frequency with temperature diminished and the Q_{10} of the pyloric frequency dropped from ~1.75 to ~1.35. Unexpectedly in Cs^+, the frequency displayed non-monotonic dynamics during temperature transitions; the frequency initially dropped as temperature increased, then rose once temperature stabilized, creating a characteristic "jag". Interestingly, these jags were still present during temperature transitions in Cs^+ when the pacemaker was isolated by picrotoxin, although the temperature-induced change in frequency recovered to control levels. Overall, these data suggest that I_h plays an important role in the ability of this circuit to produce smooth transitory responses and persistent frequency increases by different mechanisms during temperature fluctuations.

Introduction

Many repetitive motor patterns, such as breathing, walking, and swimming, operate over a wide range of frequency and relative timing of component movements (phase). The frequency and phase of these components dictates the function and efficiency of the overall motion. Many locomotor systems maintain effectiveness by changing phase concomitantly with frequency[1]. Some systems, such as lamprey[2] and leech[3] swimming, require constant phase across frequencies. In either case, when such systems transition to new steady frequencies, they normally do so in a smooth, monotonic fashion. However, control theory recognizes that while smooth transitions may be optimal, they are not inevitable. The constraints of a system can cause a non-monotonic response to a state change, in some cases even having an initial change opposite to the final appropriate response. While the dynamics of many motor patterns under stable conditions have been extensively studied, how such systems appropriately adjust their phase and frequency as conditions change and avoid turbulent dynamics has been less often addressed.

Many rhythmic neurons and muscles utilize the hyperpolarization-activated inward current, I_h, in generating their rhythmic activity[4–6]. I_h is mediated by the HCN-family of channels and is activated by hyperpolarization. This property allows excitable cells to depolarize after periods of inhibition, contributing to post-inhibitory rebound bursting behavior[4,5,7–9]. While some systems produce patterns myogenically, e.g. the vertebrate heartbeat[6,10–13], other systems rely on networks of cells to produce their activity, such as the leech heartbeat generator[14–19] or the mammalian respiratory system[20,21].

While I_h is utilized for rhythmogenesis in these systems, even a basic pattern of activity of a hard-wired neural circuit can be achieved through multiple combinations of intrinsic and

synaptic properties[22–28]. The set of properties that allow functional activity during one set of conditions is likely inadequate for all conditions. Theoretical studies suggest that parameter sets that can produce similar activity in one environment display different robustness when the environment changes[22,23]. As I_h is a key component of ubiquitous rhythmic activity, we explored its potentially changing role during transitions in conditions a rhythmic system might encounter.

To this end, we utilized the response of the pyloric rhythm of the stomatogastric ganglion (STG) of the crab, *Cancer borealis*, to temperature changes[22,29–31]. The pyloric rhythm controls food filtering by the crustacean pylorus[32]. Frequency is dictated by a three neuron electrically coupled pacemaker kernel, made up of the intrinsically oscillating anterior burster (AB) neuron and the two pyloric dilator (PD) neurons. The pacemaker kernel neurons make inhibitory synapses onto the lateral pyloric (LP) neuron and several pyloric (PY) neurons, whose properties are such that LP recovers from pacemaker inhibition before PY [29,33–35]. At ~11°C the frequency of the pyloric rhythm is typically about 1 Hz with a characteristic triphasic rhythm of activity in the PD, LP, and PY neurons[36].

As a poikilotherm, temperature changes are relevant to a crab in its natural environment. The pyloric rhythm frequency in *C. borealis* increases as temperature increases[22,30,31,37,38], but the phasing of PD, LP, and PY neurons remains constant[30,38]. Previous work has demonstrated that I_h increases in pyloric cells as temperature increases, but not whether this increase is necessary for normal responses of pyloric activity to temperature[30,39]. To probe the role I_h plays across changing conditions, we pharmacologically blocked I_h using cesium ions during temperature changes and observed the effect of this block on the frequency increase and phase constancy of the pyloric rhythm. This revealed unanticipated changes in frequency during acute transitions between temperatures.

Results

Cs^+ blocked I_h in PD and LP Neurons at 11°C and 21°C

We used 5mM CsCl in *C. borealis* saline to block I_h [39–45]. To confirm the effectiveness of this manipulation, we voltage clamped pyloric neurons (PD and LP) at the temperature extremes used in the experiment, 11°C and 21°C. We held cells at -50mV and hyperpolarized for 12s in -10mV steps from -100mV to -120mV. Because I_h is slow to activate, we quantified I_h as the difference between the initial current needed to hold the hyperpolarization and the current required to hold the hyperpolarization at steady state. At 11°C and -110mV, I_h was 1.69±0.84nA in saline and 0.4±.4nA in Cs^+, a reduction of 78±10% (3 PD cells, 2 LP cells, paired Student's t-test; p=0.0025). At 21°C and -110mV, I_h was 2.8±0.9nA in saline and 0.9±.8nA in Cs^+, a reduction of 71±20% (3 LP cells, 2 PD cells, paired Student's t-test; p=0.0011).

The steady-state frequency increase in response to elevated temperature was decreased by Cs^+

We used a combination of extracellular and intracellular recordings to monitor pyloric activity while the STG was superfused sequentially with saline or saline with 5mM CsCl. We began recording at the standard temperature of 11°C and changed the temperature of the superfused solution in steps of 2°C up to 21°C using a Peltier device. The dish temperature and pyloric activity were allowed to stabilize for 4 minutes between steps (Fig. 1A). An example of simultaneous intracellular PD and LP activity during both control saline and in Cs^+ at each temperature is shown in Fig. 1B. As previously reported[30,31,38], the pyloric frequency increased as temperature increased in control (Fig. 1B, top traces). In Cs^+ at 11°C, the pyloric frequency was significantly decreased compared to control conditions (Saline: 1.2±0.2 Hz; Cs^+ 0.9±0.2 Hz, paired Student's t-test; p<0.001) as has also been previously reported[39,44–46].

Interestingly, the degree of frequency increase with temperature was diminished in Cs^+ (Fig. 1B, bottom traces). To quantify this effect, we took the mean pyloric frequency during times when the preparation was within 0.3°C of the target temperature and plotted the mean frequency as a function of temperature (Fig. 1C). Within a preparation, the difference in frequency between control and Cs^+ at a given temperature significantly increased as temperature increased (Fig. 1D). Additionally, we characterized the temperature sensitivity of each preparation in control and Cs^+ using Q_{10} as a measure of frequency change with temperature as described previously[30]. The mean Q_{10} of the pyloric frequency was significantly lower in Cs^+ (1.3±0.5) than in control (1.7±0.3) (Fig. 1E). Together, these analyses show that the temperature-induced increase in pyloric frequency in control saline was greater than in Cs^+.

In addition to counterbalancing the starting condition, to further support the conclusion that the decline in pyloric frequency Q_{10} in Cs^+ was due to Cs^+ and not consecutive temperature changes, we performed two consecutive temperature changes in saline. The mean difference in frequency between 21°C and 11°C for the first (0.9±0.3 Hz) and second temperature changes (0.8±0.3 Hz) were not significantly different (Fig. 1F). Moreover, the mean Q_{10} of the first temperature increase (2.0±0.4) was not significantly different than the mean Q_{10} of the second temperature increase (1.8±0.4) (Fig. 1E). A two-sample t-test did not find a significant difference between the mean frequency Q_{10} in saline in experiments that underwent two saline temperature changes compared to those that experienced one in saline and one in Cs^+ (Fig. 1E). Therefore, the decrease in frequency temperature sensitivity in Cs^+ was likely not a product of sequential temperature changes.

Cs^+ revealed dynamic transitory frequency response: frequency decreased while temperature increased, then increased when temperature stabilized

While the increase in frequency over the temperature steps was primarily monotonic in control, it was often non-monotonic in Cs^+. In Cs^+, during the increases between temperatures there was often either no increase or a decrease in frequency. Figure 2 illustrates simultaneous intracellular recordings of a PD cell and an LP cell during the beginning of the step from 13°C to 15°C in both control (Fig. 2A) and Cs^+ (Fig. 2B). In control, when the temperature was increased (maroon vertical dashed line), there was a net increase in frequency. In contrast in Cs^+, there was an immediate decrease in frequency. In this particular example, the number of spikes per burst in LP decreased, though this effect was not seen in all preparations. Alignment of each PD cycle during this window to the first PD spike reveals that the decrease in frequency was due to elongation of the depolarization phase and not the bursting or repolarization phases, rather than a uniform expansion of all waveform components (Fig. 2C).

Figure 3A shows an example of the entire frequency response during a temperature step between 17°C and 19°C. In control (Fig. 3A, left), the frequency rose when the temperature increased, and stabilized when the temperature stabilized. Conversely in Cs^+, the frequency decreased when the temperature increased as in Fig. 2B, and then rose when the preparation reached the holding temperature (Fig. 3A, right). This activity produced a “jag” in the frequency-temperature curve (Fig. 3B). We compared the distributions of change in mean frequency at times when the temperature was increasing or stable across condition. “Increasing temperature” was defined as times when the change in mean temperature was greater than 0.01°C (red on Fig. 1A, 3A,B). For these increasing-temperature pyloric cycles we calculated the proportion in which the mean frequency decreased by more than 0.002 Hz (blue points in Fig. 3A; overall distribution for one experiment Fig. 3C top) in both control and Cs^+. The proportion of cycles

where frequency decreased while temperature increased was greater in Cs^+ than in control for 20 of 21 experiments. In Cs^+, the mean percent of temperature-increasing pyloric cycles in which the frequency decreased (31.4±15%) was significantly higher than in control (7.5±5%) (Fig. 3D, paired Student's t-test, N=21, p <0.001). During pyloric cycles with temperature stability (yellow on Fig. 1A, 3A,B), we calculated the proportion in which the mean frequency increased by more than 0.002 Hz (green points in Fig. 3A; overall distribution for one experiment Fig. 3C bottom). Again, this proportion was larger in Cs^+ than in control in 20 of 21 experiments. In Cs^+, the mean percent of temperature-stable cycles in which frequency increased in Cs^+ (27.6±6%) was significantly higher than in control (14.1±5%) (Fig. 3E, paired Student's t-test, N=21, p <0.001). To summarize, in Cs^+ there was a distinct tendency for the frequency to decrease when temperature increased and then increase after the temperature stabilized.

In Cs^+, follower neurons determined frequency temperature sensitivity: pacemaker kernel determined jag response

We investigated to what extent the two effects of Cs^+, change in temperature sensitivity and non-monotonic frequency response, were caused by effects in the pacemaker kernel (AB and PD neurons) versus the follower neurons (LP and PY). To do so, we repeated the temperature step protocols in control saline, 5mM Cs^+ saline, and 5mM Cs^+ + 10^{-5} picrotoxin (PTX) saline. PTX blocks the glutamatergic synapse that is the only feedback from the follower neurons to the pacemaker[31,47–49] (Fig. 4A). Figure 4B illustrates that in Cs^++PTX, the pyloric rhythm did not show the diminished frequency-increase seen in Cs^+ alone but did demonstrate jags. We compared the change in frequency between 11°C and 21°C in control, Cs^+, and Cs^++PTX and found that there was a significant effect of condition; change in frequency in Cs^+ was significantly lower than either control or Cs^++PTX (Fig. 4C) with no significant difference

between control and Cs^++PTX. Therefore, the effect of Cs^+ on the temperature-induced frequency increase appears to require the activity of the follower neurons.

We also compared the probability of frequency decrease during temperature increase and probability of frequency increase during temperature stability. Both measures showed significant effects of condition. The probability of frequency decrease while temperature increased was lower in control than in either Cs^+ or Cs^++PTX (Fig. 4D), with no difference between Cs^+ and Cs^++PTX. Interestingly, the probability of frequency increase while temperature was stable was significantly different between all three conditions: control was lowest, Cs^+ was in the middle, and Cs^++PTX was greatest. Therefore, the frequency jags appear to result from Cs^+ effects on the pacemaker kernel neurons, not the follower neurons, as they were still present when the isolated pacemaker underwent temperature steps in Cs^+.

In one experiment, the decrease in frequency while temperature increased and subsequent increase in frequency after temperature stabilized was particularly apparent in Cs^++PTX (Fig. 4F). Overlay of the PD cycles during this window aligned to the first spike again show that the decrease in frequency is due to an elongation of the depolarization phase rather than a uniform expansion of the waveform (Fig. 4G). Additionally, without the inhibition from the LP to PD synapse, the hyperpolarization associated with increased temperature[50] becomes more apparent. When in this experiment the frequency increased after temperature had stabilized, the repolarization phase shortened relative to the pre-temperature change, consistent with an overall maintenance of phase as temperature changed.

Phase of PD and LP advanced in Cs^+

We also examined the effect of Cs^+ on the firing time and phase relationships of PD, LP, and PY. Figure 5A illustrates the pyloric activity in both control (left) and Cs^+ (right) at 11°C recorded on the *pdn* (top), *lvn* (middle) and *pyn* (bottom). The time of PD bursting was significantly but modestly shorter in Cs^+ (Fig. 5B, Saline: 164±34msec, Cs^+: 144±18msec). Phase was quantified in Fig. 5C and Table 1. Given the increase in period, it follows that the phase of PD OFF (percentage of period at which PD stops firing) was significantly advanced in Cs^+ compared to control. LP onset, which follows PD offset, was also phase advanced in Cs^+ conditions compared to control. However, this phase advance was more than would be expected given respective periods and the advanced PD OFF phase, as the delay between PD OFF and LP ON phase was significantly smaller in Cs^+ compared to control (Fig. 5D, Saline: 0.21±0.06, Cs^+: 0.17±0.04).

LP OFF was also significantly advanced in Cs^+, although duty cycle (percent of the period a neuron is firing) was preserved (paired Student's t-test, N=21, p=0.448). PY ON and PY OFF were not significantly different between Cs^+ and control. The intracellular waveforms were similar between Cs^+ and control conditions apart from the noted phase-shifts. This similarity is illustrated in Fig. 5E where two cycles of each pyloric neuron's intracellular activity have been scaled to the same period.

We identified cycles where period was matched between control at 11°C and Cs^+ (typically at a higher temperature for Cs^+). Although PD burst duration was only 51±30 msec shorter in Cs^+, LP fired 91±68 msec earlier. Conversely, PY latency did not change in these matched frequency samples (1.9± 100 msec earlier). There was no correlation between how

advanced PD's offset was between control and Cs^+ conditions and how much LP's onset advanced in these matched period samples (Pearson correlation; $r(21)=0.26$, $p=0.2928$).

Phase constancy with increasing temperature was reduced by Cs^+; further advance with increasing temperatures in Cs^+

Having established that Cs^+ alters the phase relationships of PD and LP, we asked whether the phase constancy observed in control conditions in response to temperature increase was preserved in Cs^+. Figure 6A illustrates the phase of each pyloric component across temperature for both control and Cs^+ conditions. We fit a line to these points for each preparation and condition to determine as a first approximation whether there was a change in phase with temperature, though change in phase with temperature may not have been strictly linear (Fig. 6A). In control conditions, LP OFF modestly advanced with temperature, with a mean advance of 0.07±0.07 per 10°C (Wilcoxon Signed Rank test, N=21, $p<.01$). This advance is demonstrated in the two *lvn* traces in Fig. 6B, which depict one cycle of control activity at 11°C (top) and 21°C (bottom) scaled to the same period. The lilac bar highlights the advance of LP OFF at 21°C. All other pyloric components align, demonstrating phase constancy.

In Cs^+, LP ON and LP OFF advanced with temperature, with a mean advance of 0.05±0.05 per 10 °C and 0.14±0.09 per 10°C respectively (Wilcoxon Signed Rank test, N=21, $p<.01$). The advances of LP phase are shown in the two *lvn* traces in Fig. 6C, which depict one cycle of Cs^+ activity at 11°C (top) and 21°C (bottom) scaled to the same period. The purple bar highlights the LP ON advance and the lilac bar highlights the advance of LP OFF at 21°C. PD and PY phase constancy was not significantly altered in either condition. Therefore, LP phase is most sensitive to temperature and is further phase advanced by increased temperatures in Cs^+.

Discussion

Motor patterns operate over a variety of conditions with varying phase and/or frequency to meet environmental needs. While the physiological mechanisms underlying many motor patterns have been investigated under stable conditions, studies of how these mechanisms change across conditions are rarer. We investigated how I_h contributes to frequency and phase of the pyloric rhythm in *C. borealis* during temperature changes using Cs^+ to decrease I_h. We conclude I_h plays an important role in the ability of the system to appropriately adjust to temperature perturbations both transiently and persistently. Transiently, I_h removal revealed non-monotonic jags in the frequency response mediated by intrinsic properties of individual neurons. Persistently, I_h removal determined the overall frequency change (temperature sensitivity) through network effects.

The jags in frequency during transitory temperature changes upon I_h removal may be a consequence of imbalances in temperature sensitivities of individual neuron intrinsic properties

We unexpectedly found that in the presence of Cs^+, pyloric frequency decreased while temperature increased and then increased after the temperature stabilized (Figs. 2,3), producing jags in the frequency-temperature plot. This dynamic was mediated by the pacemaker alone (Fig. 4). Previous observations of the effect of temperature on pyloric frequency showed the smooth increase seen in Fig. 3A (left) and as such focused the monotonic increase of steady state response as in Fig. 1C[30,31,51]. We highlight for the first time the existence of a more dynamic response to increasing temperature. This dynamic occurred over the ~30 seconds of temperature increase and the first ~30 seconds of temperature stability (Fig. 2A(right) and Fig. 4F), suggesting the existence of a longer timescale process than previously recognized.

This longer timescale may be the result of interactions between two or more channels and/or channel-properties with fast kinetics[9,52–54]. Based on observations that the frequency decrease is associated with an elongation of the depolarization phase of a burst (Fig. 2C, 4G), we hypothesize that the decrease in frequency may be primarily caused by effects of temperature on the parameters of the transient potassium current, I_A. I_A is an inactivating, hyperpolarizing current activated by depolarization; its activation slows depolarization[30,40,55–57]. Each of its state transitions (activation, inactivation, deinactivation) may be differentially affected by temperature[30]. If deinactivation is more accelerated or altered by temperature than inactivation, then as temperature increases a larger pool of I_A channels would be available to be activated, resulting in transiently more I_A during the depolarization phase of a PD cycle. This transient increase in I_A would account for the decrease in frequency and elongated depolarization we observed. While temperature continued to change, the difference in parameters would continue to grow. Once the temperature stabilized a new equilibrium between activation, inactivation, and deinactivation could be achieved, potentially resulting in decreased total I_A during a pyloric cycle, an increase in the rate of depolarization, and an increase in frequency. I_h opposes and is correlated with I_A[25,44,55] and prevents a neuron from spending as much time in the I_A-deinactivating hyperpolarized state. Thus, when intact, we expect I_h obscures the dynamic frequency effects we propose to be caused by differential temperature sensitivities in I_A parameters.

Mathematically, activity patterns like those seen in Cs^+ where the output resulting from a step input first goes “in the wrong direction” have been described in control theory as having a “non-minimum phase dynamic”[58,59]. Typically, non-minimum phase systems are fragile and difficult to control, as they are prone to positive feedback loops unless the rate of sensor-induced

adjustment is slow. While not uncommon in physics, such dynamics are generally avoided by biological systems to ensure robust responses[59]. Our data suggest I_h plays an important role in preventing the system from producing such turbulent behavior, resulting in the typical near-instantaneous and smooth increase in frequency upon changes in temperature.

I_h dictates the steady state increase in pyloric frequency to temperature through network effects

Given that previous studies showed I_h increases in PD and LP cells at elevated temperatures[30,39], it is unsurprising that blocking I_h with Cs^+ had a larger effect at higher temperatures; the difference in I_h between control and Cs^+ is expected to be larger at elevated temperatures. As I_h is a depolarizing current, its removal would be consistent with the larger difference in frequency between saline and Cs^+ seen at higher temperatures (Fig. 1D). Unexpectedly, we found control levels of temperature-induced frequency increase in the presence of Cs^+ when the pacemaker kernel was isolated by PTX (Fig. 4 B,C). This result suggests that when temperature increases, the pacemaker kernel can increase the frequency of the pyloric rhythm without the contribution of depolarizing I_h. However, if the follower neurons can feed back to the pacemaker and I_h is blocked, the feedback limits the increase in frequency with increased temperature.

Potentially the temperature-induced increase in I_h seen in LP[30] is partially responsible for permitting the temperature-induced frequency increase seen in control conditions, and its removal by Cs^+ decreased the temperature-induced frequency increase. We noted that in Cs^+, LP phase advanced with a preserved duty cycle (Fig. 5C) and advanced further with increased temperature compared to control conditions (Fig. 6A,C). According to experiments on the effects of differently timed inhibition on pyloric frequency (phase response curve, PRC), phase advance of LP would be expected to either increase frequency have no effect[60–65], contrary to what we

observed. However, temperature-induced I_h increase in the pacemaker kernel[39] is expected to advance the PRC[46], which could permit the increase in frequency with temperature observed in control conditions despite LP inhibition. In Cs^+, this advance of the PRC would not occur[46], potentially causing the observed reduction in temperature-induced frequency increase in Cs^+ (Fig. 1B-E). In Cs^++PTX, there is no inhibition from LP to potentially slow down frequency, so compensation by increased I_h in PD would be unnecessary. Overall, while I_h is often associated with rhythmogenesis in intrinsic oscillators[4,30,66], our results demonstrate its increasing role in appropriate regulation of persistent oscillatory frequency though network feedback at elevated temperature.

LP phase in Cs^+

Surprisingly, application of Cs^+ phase advanced LP, even more than might be expected when taking into account the advance in PD offset (Fig. 5C,D). Previous studies reported no significant advance in LP, though these studies were in *Panulirus interruptus*[39,67]. Latency to LP firing increased after Cs^+ application but was insufficient to maintain or delay LP's phase given the increased period at 11°C. Increased period is known to advance LP onset[60,68,69], but our observed LP advance was maintained even in period matched samples between Cs^+ and control conditions. While in these matched samples PD bursting was shorter in Cs^+, the time by which PD offset advanced was almost half of what LP advanced and did not significantly correlate with how much LP advanced. The PD to LP synapse is depressing[70–72], such that longer recovery times between PD bursts, such as seen in period-matched Cs^+ samples, would be expected to strengthen the synapse, resulting in longer latencies to LP bursting, not shorter. Additionally, PY onset did not advance in period-matched sample. While the synapse from the pacemaker cells to

PY and LP are not the same, they have been reported to have similar properties[34] and there is no reason *a priori* to believe that Cs^+ differentially affected these synapses.

It was also surprising that when I_h was blocked, LP firing *further* advanced with temperature-mediated frequency increases. Phase maintenance is sometimes explained through a balance of synaptic depression and I_A[56,71–73]. The models of exploring phase constancy in oscillatory networks reminiscent of the STG [56,71] suggest that given I_h acts in opposition to I_A, normally I_h should impair phase constancy by *shortening* LP latencies as the period increases and advancing LP, and that this effect should be minimized when period is decreasing, such as was seen when temperature increased. By this logic, I_h removal would be expected to improve phase constancy and to have less effect on phase as period decreased, which is the opposite of what we observed. It therefore remains unclear why in Cs^+ LP was advanced and then further advanced as frequency increased with elevated temperatures.

While Cs^+ has been reported to block channels other than those responsible for I_h[20,74–78], there is no evidence that these other channels are playing significant roles in the current preparation[45]. Moreover, Cs^+ primarily blocks potassium-passing channels in a voltage dependent manner[79] such that only inward currents are blocked when Cs^+ is extracellular. Therefore, as a first approximation most of the effects seen here can likely be attributed to Cs^+ block of I_h.

Concluding remarks and general implications

There was substantial animal to animal variability in the effect of Cs^+ block of I_h. Likely this variability stems from the degeneracy in the combinations of currents that can result in a particular motor pattern[23,24,26,80–83]. Some combinations likely rely more on I_h to produce the

prototypical response to temperature. Despite this variability, without I_h, the pyloric network was unable to reliably produce either its typical rapid and smooth increase in frequency in response to temperature change, or its typical steady state increase in frequency. As such I_h may act a buffer to transient response hiccups that may be caused by intrinsic properties and as a buffer to the limiting effects of network inhibition.

Methods

Animals and Experimental Preparation

Cancer borealis were purchased from Commercial Lobster (Boston, MA) and maintained in tanks containing artificial seawater at 11°C-13°C on a 12 hr light/dark cycle for at least 1 week before use. Crabs were acquired between November 2022 and December 2023. After placing the animals on ice for 30 minutes, the stomatogastric nervous system was dissected from the crab and pinned in a petri dish coated with Sylgard (Dow Corning) as described previously[84]. All preparations included the STG, the eosophageal ganglia, and two commissural ganglia. The STGs were desheathed to allow a combination of intracellular recordings and direct solution contact with the STG. The nervous system was kept in physiological saline composed of 440 mM NaCl, 11 mM KCl, 13 mM $CaCl_2$, 26 mM $MgCl_2$, 11 mM Trizma base, and 5 mM Maleic acid, pH 7.4–7.5 at 23°C (~7.7-7.8 pH at 11°C). All reagents were purchased from Sigma.

Temperature Protocol

Temperature of superfused saline solution was controlled using a SC-20 Peltier device controlled by model CL-100 temperature controller (Warner Instruments). Temperature was monitored with a Warner Instruments TA-29 thermocouple placed within 1cm of the STG. During ‘Step’ protocols, temperature was set manually to within 0.2°C of 11°C. After 2 minutes

of recording activity, the temperature was manually increased by 2°C and allowed to stabilize over 4 minutes. This process was repeated until the dish reached 21°C, after which the temperature was returned to 11°C (Fig. 1A). The preparation was kept at 11°C for 10 minutes during which the solution was changed. Experiments started with either standard physiological saline or saline with 5mM CsCl obtained from Sigma to block I_h [39–43]. Experiments to test the importance of follower neurons in the various effects of Cs^+ were performed with first randomized Cs^+ or saline temperature steps protocol, followed by a temperature step protocol in Cs^+ + 10^{-5} M picrotoxin[49] from Sigma as picrotoxin does not easily washout.

Electrophysiology

Extracellular recordings were made by placing wells around the lower lateral ventricular nerve (*lvn*), pyloric dilator nerve (*pdn*) and pyloric constrictor nerve (*pyn*). Wells were made from 90% Vaseline 10% mineral oil solution. Stainless-steel pin electrodes were placed within the wells to monitor spiking activity and amplified using Model 3500 extracellular amplifiers (A-M Systems). Intracellular recordings from the soma of the PD, LP, and PY neurons were made using either discontinuous current clamp (one electrode) or two-electrode current and/or voltage clamp with 5-20MΩ sharp glass microelectrodes filled with 0.6 M K_2SO_4 and 20 mM KCl solution. For voltage clamp experiments, 3M KCl solutions were used to facilitate sustained current injections. Intracellular signals were amplified with an Axoclamp 900 A amplifier (Molecular Devices, San Jose). Cells were identified by matching intracellular activity with activity on the *pyn* (PY cells), *pdn* (PD cells), or *lvn* (LP cells). All amplified signals were digitized using a Digidata 1440 digitizer (Molecular Devices, San Jose) and recorded using

pClamp data acquisition software (Molecular Devices, San Jose, version 10.5), sampling frequency of 10 kHz.

Analysis

Spikes were detected and assigned to a particular neuron using a custom software implemented in MATLAB ('Crabsort', https://github.com/sg-s/crabsort)[85,86] which used a machine-learning algorithm. Results of this automated process were double checked and edited by hand. Bursts were identified as two or more consecutive PD spikes with an inter-burst interval of at least 200 msec. Phase was defined as the difference between the first spike of a PD burst and the first (onset) or last (offset) spike of a neuron (LP, PY, or PD), normalized by the period (time between first PD spikes of two consecutive bursts). Data were tested for normality using the Shapiro-Wilks Test and appropriate parametric or non-parametric tests were used.

To quantify the non-monotonic responses to temperature change, we first smoothed frequency and temperature using a moving average over 30 and 10 pyloric cycles respectively to get a less noisy trajectory for each measure. We then divided pyloric cycles based on whether the smoothed temperature increased more than 0.01°C. For cycles that increased more than this criterion, we quantified the percent in which the smoothed frequency decreased more than 0.002Hz per cycle. For cycles where temperature did not increase above the criterion, we quantified the percent in which the smoothed frequency increased more than 0.002Hz per cycle.

To examine phase constancy, we found the best fit line to describe the relationship between mean phase and temperature for each experiment. We then used either Wilcoxon Signed Rank Test (non-normal data) or one-sample t-test (normal data) to determine whether the slope

across experiments was significantly different from zero. Due to the 10 different tests (5 phases x 2 conditions), we Bonferroni-adjusted the p-values to reduce the false-positive rate.

Where not specifically noted otherwise, all summary statistic reports are (mean±SD). All analysis was performed using MATLAB.

Acknowledgements

We thank Maria Ivanova and Kathleen Jacquerie for their advice on early drafts of the manuscript. We thank Thiago Burghi, Leandro Alonso, and Kathleen Jacquerie, for their helpful discussions on dynamical systems. We would also like to thank Sonal Kedia and Margret Lee for their aid in early set up of experimental equipment.

References

1. Grillner, S. Control of Locomotion in Bipeds, Tetrapods, and Fish. in *Compr Physiol* 1179–1236 (1981). DOI: 10.1002/cphy.cp010226.

2. Cohen, A. H., Ermentrout, B. G., Kiemel, T., Kopell, N., Sigvardt, K. A. & Williams, T. L. Modelling of intersegmental coordination in the lamprey central pattern generator for locomotion. *Trends Neurosci* **15**(11) 434–438 (1992). DOI: https://doi.org/10.1016/0166-2236(92)90006-T.

3. Marder, E. & Calabrese, R. L. Principles of rhythmic motor pattern generation. *Physiol Rev* **76**(3) 687–717 (1996). DOI: 10.1152/PHYSREV.1996.76.3.687.

4. Robinson, R. B. & Siegelbaum, S. A. Hyperpolarization-Activated Cation Currents: From Molecules to Physiological Function. *Annu Rev Physiol* **65**(1) 453–480 (2003). DOI: 10.1146/annurev.physiol.65.092101.142734.

5. Biel, M., Wahl-Schott, C., Michalakis, S. & Zong, X. Hyperpolarization-Activated Cation Channels: From Genes to Function. *Physiol Rev.* **89**(3) 847–885 (2009). DOI: 10.1152/physrev.00029.2008.

6. Difrancesco, D. The Cardiac Hyperpolarizing-Activated Current, i_f. Origins and Developments. *Prog. Biophys. molec. Biol* **46** 163–183 (1985). DOI: 10.1016/0079-6107(85)90008-2.

7. Mccormick, D. A. & Pape, H.-C. Properties of a Hyperpolarzation-Activated Cation Current and its Role in Rhythmic Oscillation in Thalamic Relay Neurones. *J Physiol* **431** 291–318 (1990).

8. Mccormick, D. A. & Papet, H.-C. Noradrenergic and Serotonergic Modulation of a Hyperpolarization-Activated Cation Current in Thalalmic Relay Neurones. *J Physiol* **431** 319–342 (1990). DOI: 10.1113/jphysiol.1990.sp018332.

9. Goaillard, J. M., Taylor, A. L., Pulver, S. R. & Marder, E. Slow and persistent postinhibitory rebound acts as an intrinsic short-term memory mechanism. *J Neurosci* **30**(13) 4687–4692 (2010). DOI: 10.1523/JNEUROSCI.2998-09.2010.

10. Hagiwara, N. & Irisawa, H. Modulation by intracellular Ca^{2+} of the hyperpolarization-activated inward current in rabbit single sino-atrial node cells. *J Physiol* **409**(1) 121–141 (1989). DOI: 10.1113/JPHYSIOL.1989.SP017488.

11. Tsien, R. W., Giles, W. & Greengard, P. Cyclic AMP Mediates the Effects of Adrenaline on Cardiac Purkinji Fibres. *Nat New Biol* **240**(101) 181–183 (1972). DOI: 10.1038/newbio240181a0.

12. DiFrancesco, D. & Tromba, C. Acetylcholine inhibits activation of the cardiac hyperpolarizing-activated current, $i_{,f}$. *Pflugers Arch* **410**(1–2) 139–142 (1987). DOI: 10.1007/BF00581906.

13. Yanagihara, K. & Irisawa, H. Inward current activated during hyperpolarization in the rabbit sinoatrial node cell. *Pflugers Arch* **385**(1) 11–19 (1980). DOI: 10.1007/BF00583909.

14. Nadim, F., Olsen, Ø. H., de Schutter, E. & Calabrese, R. L. Modeling the leech heartbeat elemental oscillator I. Interactions of intrinsic and synaptic currents. *J Computational Neuro* **2**(3) 215–235 (1995). DOI: 10.1007/BF00961435.

15. Angstadt, J. D. & Calabrese, R. L. A hyperpolarization-activated inward current in heart interneurons of the medicinal leech. *J Neurosci* **9**(8) 2846–2857 (1989). DOI: 10.1523/jneurosci.09-08-02846.1989.

16. Calabrese, R. L., Nadim, F. & Olsen, Ø. H. Heartbeat control in the medicinal leech: A model system for understanding the origin, coordination, and modulation of rhythmic motor patterns. *J Neurobio* **27**(3) 390–402 (1995). DOI: 10.1002/neu.480270311.

17. Wenning, A., Cymbalyuk, G. S. & Calabrese, R. L. Heartbeat Control in Leeches. I. Constriction Pattern and Neural Modulation of Blood Pressure in Intact Animals. *J Neurophysiol* **91**(1) 382–396 (2004). DOI: 10.1152/jn.00526.2003.

18. Stent, G. S., Thompson, W. J. & Calabrese, R. L. Neural Control of Heartbeat in the Leech and in Some Other Invertebrates. *Physiol Rev* **59**(1) 101–136 (1979).

19. Tobin, A. E. & Calabrese, R. L. Myomodulin increases I_h and inhibits the Na/K pump to modulate bursting in leech heart interneurons. *J Neurophysiol* **94**(6) 3938–3950 (2005). DOI: 10.1152/jn.00340.2005.

20. Thoby-Brisson, M., Telgkamp, P. & Ramirez, J. M. The role of the hyperpolarization-activated current in modulating rhythmic activity in the isolated respiratory network of mice. *J Neurosci* **20**(8) 2994–3005 (2000). DOI: 10.1523/jneurosci.20-08-02994.2000.

21. Thoby-Brisson, M., Cauli, B., Champagnat, J., Fortin, G. & Katz, D. M. Expression of functional Tyrosine kinase B receptors by rhythmically active respiratory neurons in the pre-Bötzinger complex of neonatal mice. *J Neurosci* **23**(20) 7685–7689 (2003). DOI: 10.1523/jneurosci.23-20-07685.2003.

22. Alonso, L. M. & Marder, E. Temperature compensation in a small rhythmic circuit. *Elife* **9** e55470 (2020). DOI: 10.7554/eLife.55470.

23. Alonso, L. M. & Marder, E. Visualization of currents in neural models with similar behavior and different conductance densities. *Elife* **8** e42722 (2019). DOI: 10.7554/eLife.42722.

24. Schulz, D. J., Goaillard, J. M. & Marder, E. Variable channel expression in identified single and electrically coupled neurons in different animals. *Nat Neurosci* **9**(3) 356–362 (2006). DOI: 10.1038/nn1639.

25. Schulz, D. J., Goaillard, J. M. & Marder, E. E. Quantitative expression profiling of identified neurons reveals cell-specific constraints on highly variable levels of gene expression. *Proc Natl Acad Sci U S A* **104**(32) 13187–13191 (2007). DOI: 10.1073/pnas.0705827104.

26. Prinz, A. A., Bucher, D. & Marder, E. Similar network activity from disparate circuit parameters. *Nat Neurosci* **7**(12) 1345–1352 (2004). DOI: 10.1038/nn1352.

27. Golowasch, J., Abbott, L. F. & Marder, E. Activity-dependent regulation of potassium currents in an identified neuron of the stomatogastric ganglion of the crab *Cancer borealis*. *J Neurosci* **19**(20) RC33 (1999). DOI: 10.1523/jneurosci.19-20-j0004.1999.

28. Golowasch, J., Casey, M., Abbott, L. F. & Marder, E. Network stability from activity-dependent regulation of neuronal conductances. *Neural Comput* **11**(5) 1079–1096 (1999). DOI: 10.1162/089976699300016359.

29. Marder, E. & Bucher, D. Understanding circuit dynamics using the stomatogastric nervous system of lobsters and crabs. *Annu Rev Physiol* **69** 291–316 (2007). DOI: 10.1146/annurev.physiol.69.031905.161516.

30. Tang, L. S., Goeritz, M. L., Caplan, J. S., Taylor, A. L., Fisek, M. & Marder, E. Precise temperature compensation of phase in a rhythmic motor pattern. *PLoS Biol* **8**(8) 21–22 (2010). DOI: 10.1371/journal.pbio.1000469.

31. Rinberg, A., Taylor, A. L. & Marder, E. The Effects of Temperature on the Stability of a Neuronal Oscillator. *PLoS Comput Biol* **9**(1) e1002857 (2013). DOI: 10.1371/journal.pcbi.1002857.

32. McGaw, I. J. & Curtis, D. L. A review of gastric processing in decapod crustaceans. *J Comp Physiol B* **183**(4) 443–465 (2013). DOI: 10.1007/s00360-012-0730-3.

33. Hartline, D. K. Pattern generation in the lobster (*Panulirus*) stomatogastric ganglion - II. Pyloric network simulation. *Biol Cybern* **33**(4) 223–236 (1979). DOI: 10.1007/BF00337411.

34. Rabbah, P. & Nadim, F. Synaptic dynamics do not determine proper phase of activity in a central pattern generator. *J Neurosci* **25**(49) 11269–11278 (2005). DOI: 10.1523/JNEUROSCI.3284-05.2005.

35. Hartline, D. K. & Gassie, D. V. Pattern generation in the lobster (*Panulirus*) stomatogastric ganglion - I. Pyloric neuron kinetics and synaptic interactions. *Biol Cybern* **33**(4) 209–222 (1979). DOI: 10.1007/BF00337410.

36. Hamood, A. W., Haddad, S. A., Otopalik, A. G., Rosenbaum, P. & Marder, E. Quantitative Reevaluation of the Effects of Short- and Long-Term Removal of Descending Modulatory Inputs on the Pyloric Rhythm of the Crab, Cancer borealis. *eNeuro* **2**(1) 58–72 (2015). DOI: 10.1523/ENEURO.0058-14.2015.

37. Haddad, S. A. & Marder, E. Circuit Robustness to Temperature Perturbation Is Altered by Neuromodulators. *Neuron* **100**(3) 609-623.e3 (2018). DOI: 10.1016/J.NEURON.2018.08.035.

38. Soofi, W., Goeritz, M. L., Kispersky, T. J., Prinz, A. A., Marder, E. & Stein, W. Phase maintenance in a rhythmic motor pattern during temperature changes in vivo. *J Neurophysiol* **111**(12) 2603–2613 (2014). DOI: 10.1152/jn.00906.2013.

39. Peck, J. H., Gaier, E., Stevens, E., Repicky, S. & Harris-Warrick, R. M. Amine modulation of Ih in a small neural network. *J Neurophysiol* **96**(6) 2931–2940 (2006). DOI: 10.1152/jn.00423.2005.

40. Harris-Warrick, R. M., Coniglio, L. M., Barazangi, N., Guckenheimer, J. & Gueron, S. Dopamine modulation of transient potassium current evokes phase shifts in a central pattern generator network. *J Neurosci* **15**(1 I) 342–358 (1995). DOI: 10.1523/jneurosci.15-01-00342.1995.

41. Harris-Warrick, R., Coniglio, L. M., Levini, R. M., Gueron, S. & Guckenheimer, J. Dopamine Modulation of Two Subthreshold Currents Produces Phase Shifts in Activity of an Identified Motoneuron. *J Neurophysiol* **74**(4) 1404–1420 (1995). DOI: 10.1152/jn.1995.74.4.1404.

42. Goeritz, M. L., Ouyang, Q. & Harris-Warrick, R. M. Localization and function of I_h channels in a small neural network. *J Neurophysiol* **106** 44–58 (2011). DOI: 10.1152/jn.00897.2010.-Sub.

43. Ballo, A. W., Keene, J. C., Troy, P. J., Goeritz, M. L., Nadim, F. & Bucher, D. Dopamine modulates I_h in a motor axon. *J Neurosci* **30**(25) 8425–8434 (2010). DOI: 10.1523/JNEUROSCI.0405-10.2010.

44. Zhang, Y., Oliva, R., Gisselmann, G., Hatt, H., Guckenheimer, J. & Harris-Warrick, R. M. Overexpression of a Hyperpolarization-Activated Cation Current (I_h) Channel Gene Modifies the Firing Activity of Identified Motor Neurons in a Small Neural Network. *J Neurosci* **23**(27) 9059–9067 (2003). DOI: 10.1523/JNEUROSCI.23-27-09059.2003.

45. Zhu, L., Selverston, A. I. & Ayers, J. Role of I_h in differentiating the dynamics of the gastric and pyloric neurons in the stomatogastric ganglion of the lobster, *Homarus americanus*. *J Neurophysiol* **115**(5) 2434–2445 (2016). DOI: 10.1152/JN.00737.2015.

46. Soofi, W. & Prinz, A. A. Differential effects of conductances on the phase resetting curve of a bursting neuronal oscillator. *J Comput Neurosci* **38**(3) 539–558 (2015). DOI: 10.1007/S10827-015-0553-9/TABLES/3.

47. Eisen, J. S. & Marder, E. A mechanism for production of phase shifts in a pattern generator. *J Neurophysiol* **51**(6) 1375–1393 (1984). DOI: 10.1152/JN.1984.51.6.1375.

48. Eisen, J. S. & Marder, E. Mechanisms underlying pattern generation in lobster stomatogastric ganglion as determined by selective inactivation of identified neurons. III. Synaptic connections of electrically coupled pyloric neurons. *J. Neurophysiol* **48**(6) 1392–1415 (1982). DOI: 10.1152/JN.1982.48.6.1392.

49. Bidaut, M. Pharmacological dissection of pyloric network of the lobster stomatogastric ganglion using picrotoxin. *J. Neurophysiol.* **44**(6) 1089–1101 (1980). DOI: 10.1152/JN.1980.44.6.1089.

50. Morozova, E., Newstein, P. & Marder, E. Reciprocally inhibitory circuits operating with distinct mechanisms are differently robust to perturbation and modulation. *Elife* **11** (2022). DOI: 10.7554/ELIFE.74363.

51. Marder, E. & Rue, M. C. P. From the Neuroscience of Individual Variability to Climate Change. *J. Neuroscie* **41**(50) 10213–10221 (2021). DOI: 10.1523/JNEUROSCI.1261-21.2021.

52. Connor, J. A. Neural repetitive firing: a comparative study of membrane properties of crustacean walking leg axons. *J. Neurophysiol* **38**(4) 922–932 (1975). DOI: 10.1152/JN.1975.38.4.922.

53. Connor, J. A. Slow repetitive activity from fast conductance changes in neurons. *Fed Proc* **37**(8) 2139–2145 (1978).

54. Connor, J. A., Walter, D. & Mckown, R. Neural repetitive firing: modifications of the Hodgkin-Huxley axon suggested by experimental results from crustacean axons. *Biophys J.* **18**(1) 81–102 (1977). DOI: 10.1016/S0006-3495(77)85598-7.

55. MacLean, J. N., Zhang, Y., Goeritz, M. L., Casey, R., Oliva, R., Guckenheimer, J. & Harris-Warrick, R. M. Activity-independent coregulation of I_A and I_h in rhythmically active neurons. *J Neurophysiol* **94**(5) 3601–3617 (2005). DOI: 10.1152/jn.00281.2005.

56. Greenberg, I. & Manor, Y. Synaptic Depression in Conjunction With A-Current Channels Promote Phase Constancy in a Rhythmic Network. *J Neurophysiol* **93**(2) 656–677 (2005). DOI: 10.1152/jn.00640.2004.

57. Tierney, A. J. & Harris-Warrick, R. M. Physiological role of the transient potassium current in the pyloric circuit of the lobster stomatogastric ganglion. *J Neurophysiol* **67**(3) 599–609 (1992). DOI: 10.1152/JN.1992.67.3.599.

58. Franklin, G. F., Powell, J. D. & Emami-Naeini. *Feedback Control of Dynamic Systems, Vol. 7.* (2002).

59. Khammash, M. An engineering viewpoint on biological robustness. *BMC Biol* **14**(1) 22 (2016). DOI: 10.1186/s12915-016-0241-x.

60. Mamiya, A. & Nadim, F. Dynamic Interaction of Oscillatory Neurons Coupled with Reciprocally Inhibitory Synapses Acts to Stabilize the Rhythm Period. *J Neurosci* **24**(22) 5140–5150 (2004). DOI: 10.1523/JNEUROSCI.0482-04.2004.

61. Nadim, F., Zhao, S., Zhou, L. & Bose, A. Inhibitory feedback promotes stability in an oscillatory network. *J Neural Eng* **8**(6) 065001 (2011). DOI: 10.1088/1741-2560/8/6/065001.

62. Weaver, A. L. & Hooper, S. L. Follower Neurons in Lobster (*Panulirus interruptus*) Pyloric Network Regulate Pacemaker Period in Complementary Ways. *J Neurophysiol* **89**(3) 1327–1338 (2003). DOI: 10.1152/jn.00704.2002.

63. Thirumalai, V., Prinz, A. A., Johnson, C. D. & Marder, E. Red pigment concentrating hormone strongly enhances the strength of the feedback to the pyloric rhythm oscillator but has little effect on pyloric rhythm period. *J Neurophysiol* **95**(3) 1762–1770 (2006). DOI: 10.1152/jn.00764.2005.

64. Johnson, B. R., Brown, J. M., Kvarta, M., Lu, J., Schneider, L. R., Nadim, F. & Harris-Warrick, R. M. Differential Modulation of Synaptic Strength and Timing Regulate Synaptic Efficacy in a Motor Network. *J Neurophysiol* **105**(1) 293–304 (2010). DOI: 10.1152/jn.00809.2010.

65. Hooper, R. M., Tikidji-Hamburyan, R. A., Canavier, C. C. & Prinz, A. A. Feedback control of variability in the cycle period of a central pattern generator. *J Neurophysiol* **114**(5) 2741–2752 (2015). DOI: 10.1152/jn.00365.2015.

66. Brown, H. F., Difrancesco, D. & Noble, S. J. How does adrenaline accelerate the heart? [13]. *Nature* **280**(5719) 235–236 (1979). DOI: 10.1038/280235a0.

67. Rodgers, E. W., Fu, J. J., Krenz, W. D. C. & Baro, D. J. Tonic nanomolar dopamine enables an activity-dependent phase recovery mechanism that persistently alters the maximal conductance of the hyperpolarization-activated current in a rhythmically active neuron. *J Neurosci* **31**(45) 16387–16397 (2011). DOI: 10.1523/JNEUROSCI.3770-11.2011.

68. Hooper, S. L. Phase Maintenance in the Pyloric Pattern of the Lobster (*Panulirus interruptus*) Stomatogastric Ganglion. *J Comput Neurosci* **4** 191–205 (1997). DOI: 10.1023/a:1008822218061.

69. Martinez, D., Anwar, H., Bose, A., Bucher, D. M. & Nadim, F. Short-term synaptic dynamics control the activity phase of neurons in an oscillatory network. *Elife* **8** e46911 (2019). DOI: 10.7554/ELIFE.46911.

70. Manor, Y., Nadim, F., Abbott, L. F. & Marder, E. Temporal Dynamics of Graded Synaptic Transmission in the Lobster Stomatogastric Ganglion. *J Neurosci* **17**(14) 5610–5621 (1997). DOI: 10.1523/JNEUROSCI.17-14-05610.1997.

71. Manor, Y., Bose, A., Booth, V. & Nadim, F. Contribution of Synaptic Depression to Phase Maintenance in a Model Rhythmic Network. *J Neurophysiol* **90**(5) 3513–3528 (2003). DOI: 10.1152/jn.00411.2003.

72. Mouser, C., Nadim, F. & Bose, A. Maintaining phase of the crustacean tri-phasic pyloric rhythm. *J Math Biol* **57**(2) 161–181 (2008). DOI: 10.1007/S00285-007-0150-2.

73. Bose, A., Manor, Y. & Nadim, F. The activity phase of postsynaptic neurons in a simplified rhythmic network. *J Comput Neurosci* **17**(2) 245–261 (2004). DOI: 10.1023/B:JCNS.0000037685.71759.1A.

74. Pape, H.-C. Queer Current and Pacemaker: The Hyperpolarization-Activated Cation Current in Neurons. *Annu Rev. Phyiol* **58** 299–327 (1996).

75. Wischmeyer, E. & Karschin, A. A novel slow hyperpolarization-activated potassium current (IK(SHA)) from a mouse hippocampal cell line. *J Physiol* **504**(Pt 3) 591–602 (1997). DOI: 10.1111/J.1469-7793.1997.591BD.X.

76. Coggan, J. S., Purnyn, S. L., Knoper, S. R. & Kreulen, D. L. Muscarinic inhibition of two potassium currents in guinea-pig prevertebral neurons: Differentiation by extracellular cesium. *Neuroscience* **59**(2) 349–361 (1994). DOI: 10.1016/0306-4522(94)90601-7.

77. Harding, S. D., Armstrong, J. F., Faccenda, E., Southan, C., Alexander, S. P. H., Davenport, A. P., Spedding, M. & Davies, J. A. The IUPHAR/BPS Guide to Pharmacology in 2024. *Nucleic Acids Res* **52**(D1) D1438–D1449 (2023). DOI: 10.1093/nar/gkad944.

78. Brown, D. A. & Adams, P. R. Muscarinic suppression of a novel voltage-sensitive K^+ current in a vertebrate neurone. *Nature* **283**(5748) 673–676 (1980). DOI: 10.1038/283673a0.

79. Clay, J. R. & Shlesinger, M. F. Analysis of the effects of cesium ions on potassium channel currents in biological membranes. *J Theor Biol* **107**(2) 189–201 (1984). DOI: 10.1016/S0022-5193(84)80021-1.

80. Krenz, W.-D. C., Rodgers, E. W. & Baro, D. J. Tonic 5nM DA Stabilizes Neuronal Output by Enabling Bidirectional Activity-Dependent Regulation of the Hyperpolarization Activated Current via PKA and Calcineurin. *PLoS One* **10**(2) e0117965 (2015). DOI: 10.1371/journal.pone.0117965.

81. Goaillard, J. M., Taylor, A. L., Schulz, D. J. & Marder, E. Functional consequences of animal-to-animal variation in circuit parameters. *Nat Neurosci* **12**(11) 1424–1430 (2009). DOI: 10.1038/NN.2404.

82. Anwar, H., Martinez, D., Bucher, D. & Nadim, F. Inter-Animal Variability in Activity Phase Is Constrained by Synaptic Dynamics in an Oscillatory Network. *eNeuro* **9**(4) ENEURO.0027-22.2022 (2022). DOI: 10.1523/ENEURO.0027-22.2022.

83. Marder, E., Kedia, S. & Morozova, E. O. New insights from small rhythmic circuits. *Curr Opin Neurobiol* **76** 102610 (2022). DOI: 10.1016/J.CONB.2022.102610.

84. Gutierrez, G. J. & Grashow, R. G. *Cancer borealis* stomatogastric nervous system dissection. *J Visualized Experiments* **25** 1207 (2009). DOI: 10.3791/1207.

85. Powell, D., Haddad, S. A., Gorur-Shandilya, S. & Marder, E. Coupling between fast and slow oscillator circuits in cancer borealis is temperature-compensated. *Elife* **10** 1–23 (2021). DOI: 10.7554/ELIFE.60454.

86. Gorur-Shandilya, S., Cronin, E. M., Schneider, A. C., Haddad, S. A., Rosenbaum, P., Bucher, D., Nadim, F. & Marder, E. Mapping circuit dynamics during function and dysfunction. *Elife* **11** (2022). DOI: 10.7554/elife.76579.

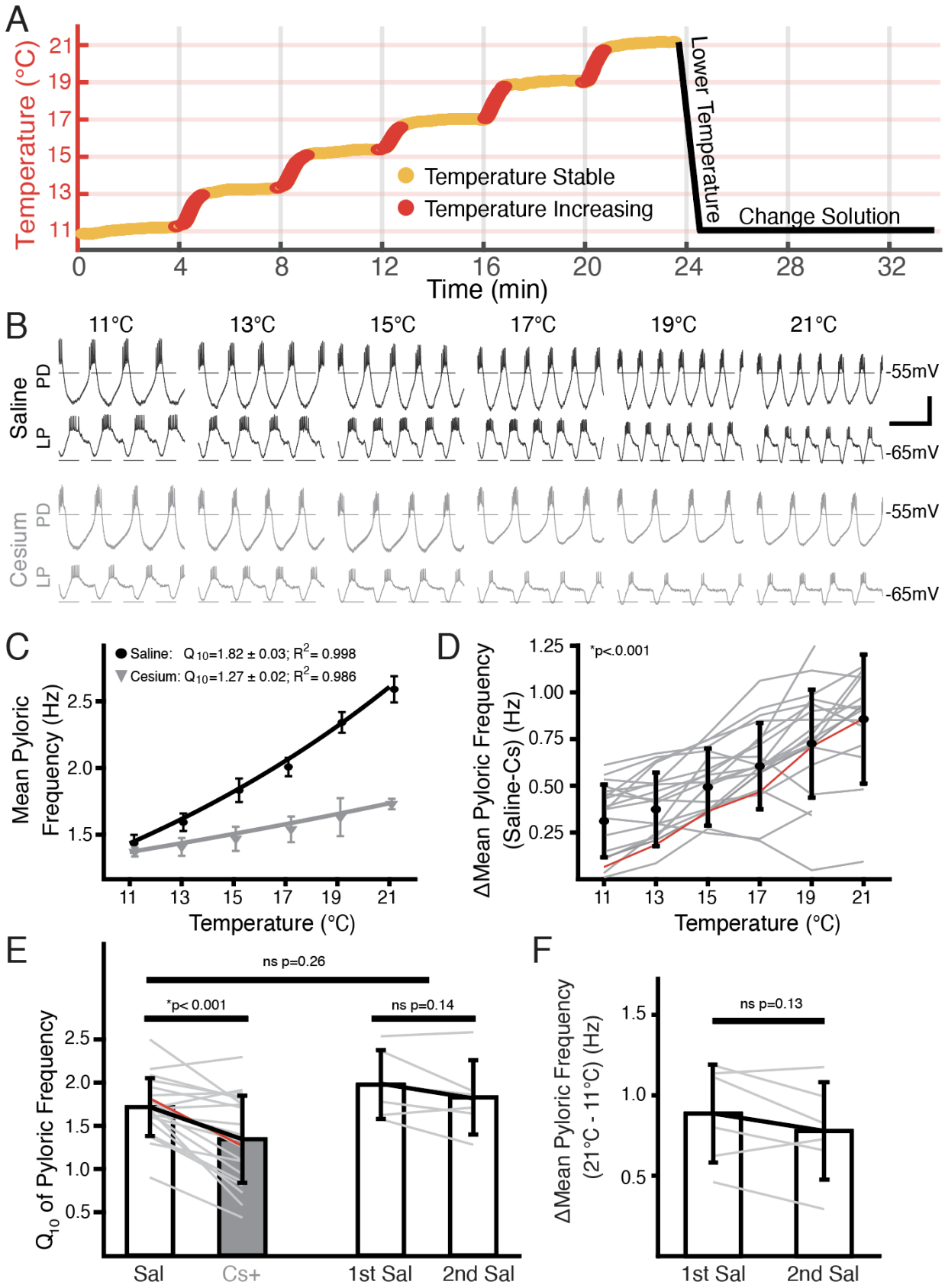
A
Temperature (°C)
21
19
17
15
13
11
Temperature Stable
Temperature Increasing
Lower Temperature
Change Solution
0
4
8
12
16
20
24
28
32
Time (min)
B
11°C
13°C
15°C
17°C
19°C
21°C
Saline
PD
LP
-55mV
-65mV
Cesium
PD
LP
-55mV
-65mV
C
Saline: Q10=1.82 ± 0.03; R2= 0.998
Cesium: Q10=1.27 ± 0.02; R2= 0.986
Mean Pyloric Frequency (Hz)
2.5
2.0
1.5
11
13
15
17
19
21
Temperature (°C)
D
*p<.0.001
ΔMean Pyloric Frequency (Saline-Cs) (Hz)
1.25
1.00
0.75
0.50
0.25
11
13
15
17
19
21
Temperature (°C)
E
ns p=0.26
*p< 0.001
ns p=0.14
Q10 of Pyloric Frequency
2.5
2.0
1.5
1.0
0.5
Sal
Cs+
1st Sal
2nd Sal
F
ns p=0.13
ΔMean Pyloric Frequency (21°C - 11°C) (Hz)
1.5
1.0
0.5
1st Sal
2nd Sal

Figures

Figure 1: Temperature-induced frequency increase was diminished by Cs^+ application. **(A)** Basic experimental protocol. Experiment began in saline or Cs^+ solution (order randomized) at 11°C. The superfusion solution temperature was changed in steps of 2°C and allowed to stabilize over 4 minutes. Red represents times when the temperature was increasing, yellow when the temperature was considered stable. After the holding period at 21°C the preparation was returned to 11°C. The solution was then changed to the remaining condition over 10 minutes and the step protocol was repeated. **(B)** Intracellular recordings from a single preparation while in saline (**top**) and Cs^+ (**bottom**) at each holding temperature (yellow in **A**) from 11°C to 21°C. Within a condition the top trace is PD and the bottom trace is LP. Burst frequency increased as temperature increased in saline, but less so in Cs^+. Scalebar: Horizontal=1s, Vertical=20mV. **(C)** Mean frequency ± SD at each holding temperature across conditions from a different preparation than in **B**. Line represents the best fit Q_{10} equations for each condition; preparation in saline had a larger Q_{10} than in Cs^+ and as such a larger frequency increase with temperature. **(D)** Mean ± SD difference in frequency between saline and Cs^+ across temperatures and preparations. As temperature increased, the difference between a preparation's frequency in saline and Cs^+ significantly increased (1-way repeated measures ANOVA ($F(5,85) = 43.259$, $p < 0.001$, N = 21). Grey lines represent individual experiments, red line represents experiment depicted in **C**. **(E)** Q_{10} was significantly lower in Cs^+ than in saline (paired Student's t-test, $p < 0.001$, N=21). Q_{10} was not significantly different in two consecutive saline temperature changes (paired Student's t-test, $p = 0.14$, N=6). Q_{10} was also not significantly different between the mean Q_{10} of the experiments with two saline temperature changes those that experienced one saline and one Cs^+ temperature change (two-sample t-test, $p=0.26$). Bars are mean ± SD, individual lines represent individual experiments, red line is experiment depicted in **C**. **(F)** Overall change in mean pyloric frequency from 11°C to 21°C was not significantly different between first and second temperature change in saline (paired Student's t-test, $p=0.14$, N=6).

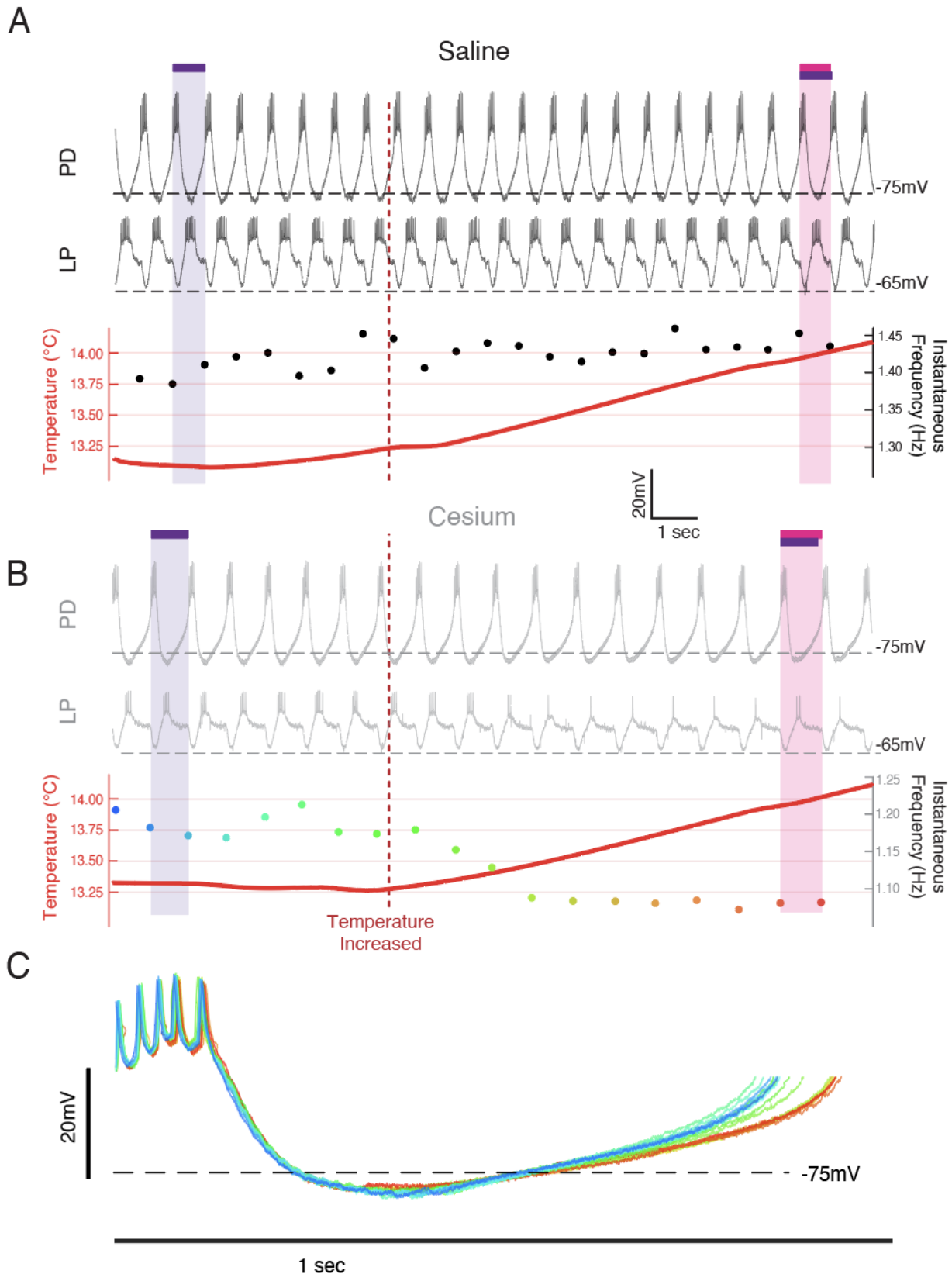
A
Saline
PD
LP
-75mV
-65mV
Temperature (°C)
14.00
13.75
13.50
13.25
Instantaneous Frequency (Hz)
1.45
1.40
1.35
1.30
20mV
1 sec
Cesium
B
PD
LP
-75mV
-65mV
Temperature (°C)
14.00
13.75
13.50
13.25
Instantaneous Frequency (Hz)
1.25
1.20
1.15
1.10
Temperature Increased
C
20mV
-75mV
1 sec

Figure 2: Frequency decreased when temperature was increased in Cs^+ through an elongation of the depolarization phase. Example from a single preparation as temperature was changed from 13°C towards 15°C in Saline**(A)** and Cs^+**(B,C)**. **(A,B) Top:** the intracellular recording from PD; **Middle:** simultaneous intracellular recording from LP; **Bottom:** simultaneous temperature (red; left axis) and instantaneous frequency (right axis). Purple bar highlights one pyloric period before the temperature was increased, while the magenta bar highlights one pyloric period after. (**A**) In saline when the temperature increased (maroon line), the period decreased as highlighted by the magenta bar being shorter than the purple bar. (**B**) In Cs^+, the period increased after the temperature shift, as highlighted by the magenta bar being longer than the purple bar. The same scale is used in both **A** and **B**. (**C**) Individual PD cycles from **B** aligned to the first spike. Coloration indicates when an individual cycle occurred as keyed by the instantaneous frequency trace in **B**. Increased period corresponds to an elongation of the depolarization phase and a maintenance of the bursting and repolarization phases.

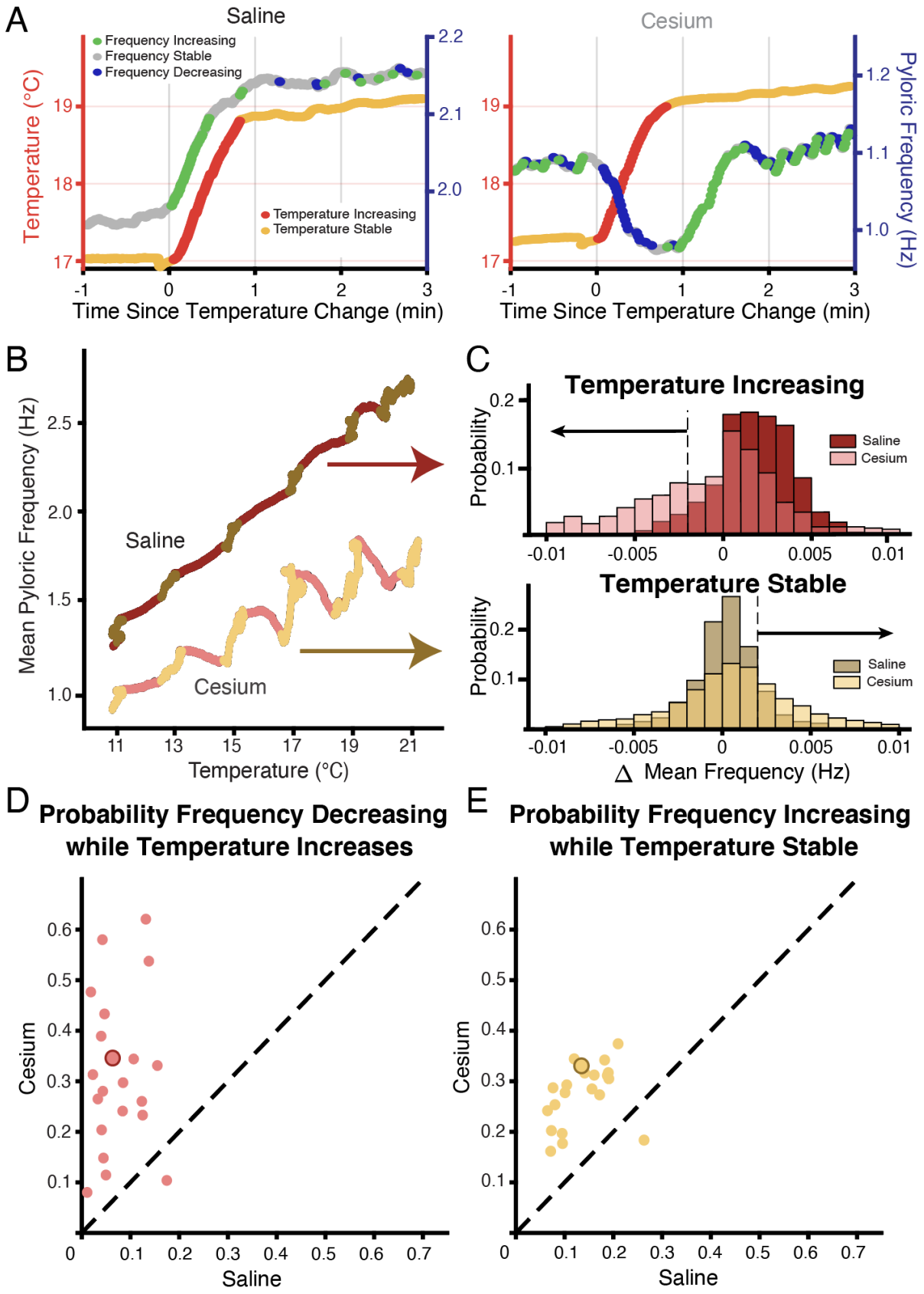
A
Saline
Cesium
Frequency Increasing
Frequency Stable
Frequency Decreasing
Temperature Increasing
Temperature Stable
Temperature (°C)
Pyloric Frequency (Hz)
Time Since Temperature Change (min)
B
Mean Pyloric Frequency (Hz)
Saline
Cesium
Temperature (°C)
C
Temperature Increasing
Temperature Stable
Probability
Saline
Cesium
Δ Mean Frequency (Hz)
D
Probability Frequency Decreasing while Temperature Increases
E
Probability Frequency Increasing while Temperature Stable
Cesium
Saline

Figure 3: Across preparations frequency was more likely to decrease when temperature increased and increase when temperature was stable in Cs^+ compared to saline. **(A)** Example of a temperature step from 17°C to 19°C in saline **(left)** and Cs^+ **(right)**. Left axis and warm colors denote temperature, with reds denoting temperature increasing by more than 0.01°C/pyloric cycle, and yellows denoting stable temperature (change less than 0.01°C/pyloric cycle). Right axis and cool colors denote frequency, with green indicating mean frequency increase >0.002 Hz, blue indicating mean frequency decrease >0.002 Hz, and grey stable frequency between these bounds. In saline, frequency change closely mirrored temperature change. In Cs^+, frequency decreased (blue) when temperature increased (red) and increased (green) when temperature stabilized (yellow). **(B)** Mean pyloric frequency as a function of temperature for a single experiment in both saline and Cs^+. Note how in saline the frequency increased largely monotonically along the entire temperature range, increasing most when temperature increased (maroon). Conversely in Cs^+ the frequency displayed a non-monotonic, sawtooth-like pattern, decreasing when temperature increased (pink) and increasing when temperature was stable (light yellow). **(C)** For the same experiment as in **B**, distribution of mean change in frequency for cycles when the mean temperature was increasing (**top**) or when the temperature was stable (**bottom**), definition of temperature same as in **A**,**B**, Fig. 1A. When the temperature increased, the change in mean frequency was more likely decrease Cs^+ than in saline. When temperature was stable, the change in mean frequency was more likely to increase in Cs^+ than in saline. Black arrows highlight the range used for frequency color coding in **A** and quantification in **D** and **E**. **(D)** Across experiments, the probability of decreasing mean frequency while temperature increased in Cs^+ or in saline. For 20/21 of experiments, the probability was higher in Cs^+ than saline. Experiment from **B,C** is highlighted by the larger, outlined point. **(E)** Across experiments, the probability of having an increasing frequency while temperature was stable. For 20/21 of experiments, the probability was higher in Cs^+ than saline. Again, experiment from **B,C** is highlighted by the larger, outlined point.

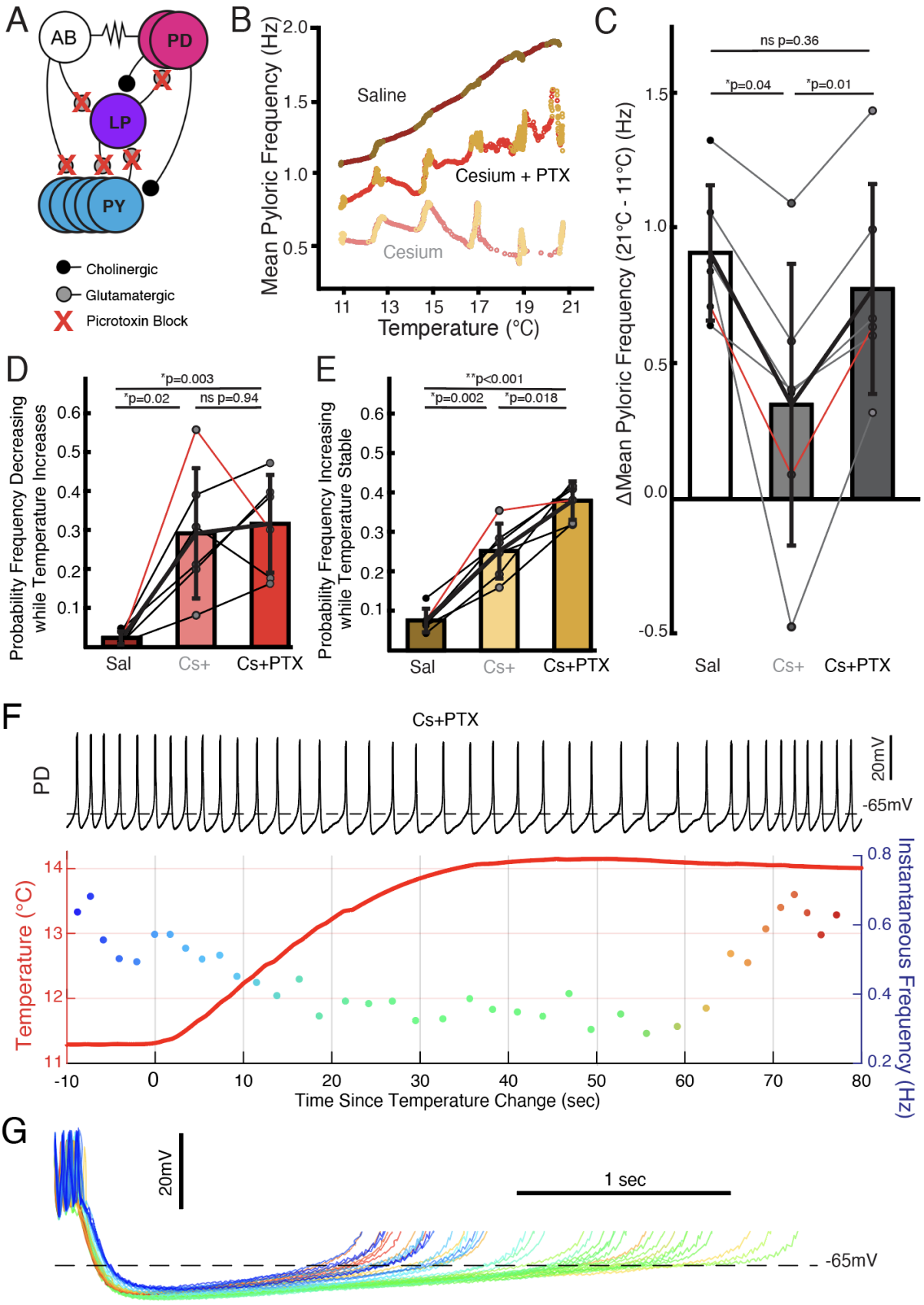
A
AB
PD
LP
PY
Cholinergic
Glutamatergic
Picrotoxin Block
B
Mean Pyloric Frequency (Hz)
Saline
Cesium + PTX
Cesium
Temperature (°C)
C
ΔMean Pyloric Frequency (21°C - 11°C) (Hz)
ns p=0.36
*p=0.04
*p=0.01
Sal
Cs+
Cs+PTX
D
Probability Frequency Decreasing while Temperature Increases
*p=0.003
*p=0.02
ns p=0.94
E
Probability Frequency Increasing while Temperature Stable
**p<0.001
*p=0.002
*p=0.018
F
Cs+PTX
PD
20mV
-65mV
Temperature (°C)
Instantaneous Frequency (Hz)
Time Since Temperature Change (sec)
G
20mV
1 sec
-65mV

Figure 4: Follower neurons mediated pyloric frequency temperature sensitivity change by Cs^+, while non-monotonic temperature response was mediated by the pacemaker kernel neurons. **(A)** Wiring diagram of the pyloric network, illustrating the pacemaker kernel neurons (AB and PD) and the follower neurons (LP and PY). The only feedback synapse to the pacemaker kernel neurons, LP to PD, and is blocked by picrotoxin (PTX). **(B)** Mean pyloric frequency as a function of temperature for a single experiment in saline, Cs^+, and Cs^+ + PTX. Reds denote temperature increasing by more than 0.01°C/cycle, yellows denote stable temperature (change less than 0.01°C/cycle). In Cs^+ + PTX, the steady-state increase in frequency (yellows) as a function of temperature was similar to saline (trajectory roughly parallel). However, in Cs^+ + PTX pyloric frequency displayed non-monotonic responses to periods of transitory temperature increase as in Cs^+ alone. **(C)** There was a significant effect of condition on the change in frequency between 11°C and 21°C for N=6 experiments as a measure of temperature sensitivity (one-way repeated measures ANOVA; $F(2,10)=12.272$, $p=0.002$). Post hoc Tukey's Honestly Significant Difference (HSD) indicated the frequency changed significantly less in Cs^+ alone compared to either control or Cs^+ + PTX. Experiment from **B** is highlighted in red. **(D)** There was a significant effect of condition on the probability of frequency decrease during periods of temperature increase for N=6 experiments (one-way repeated measures ANOVA; $F(2,10)=13.077$, $p=0.002$). HSD indicated the probability was significantly higher in both Cs^+ and Cs^+ + PTX compared to control. Experiment from **B** is highlighted in red. **(E)** There was a significant effect of condition on the probability of frequency increase during periods of temperature stability for N=6 experiments (one-way repeated measures ANOVA; $F(2,10)=69.572$, $p < 0.001$). HSD indicated the probability was significantly greater Cs^+ than control and significantly greater in Cs^+ + PTX than in Cs^+. Experiment from **B** is highlighted in red. This elevated probability of increase may partially account for the lack of overall temperature-sensitivity decrease in Cs^++ PTX compared to Cs^+ alone in **C**. (**F)** Same scheme as Fig. 2B and C. In Cs^+ + PTX frequency decreased when temperature rose and eventually increased once temperature stabilized. **(G)** Individual cycles from **F** aligned to the first spike, colored as in the instantaneous frequency trace in **F**. When the temperature increased (greenish traces), the depolarization phase dramatically elongated and there was some increased hyperpolarization. After approximately 30 seconds of stable temperature, frequency increased and the depolarization accelerated again (reddish traces).

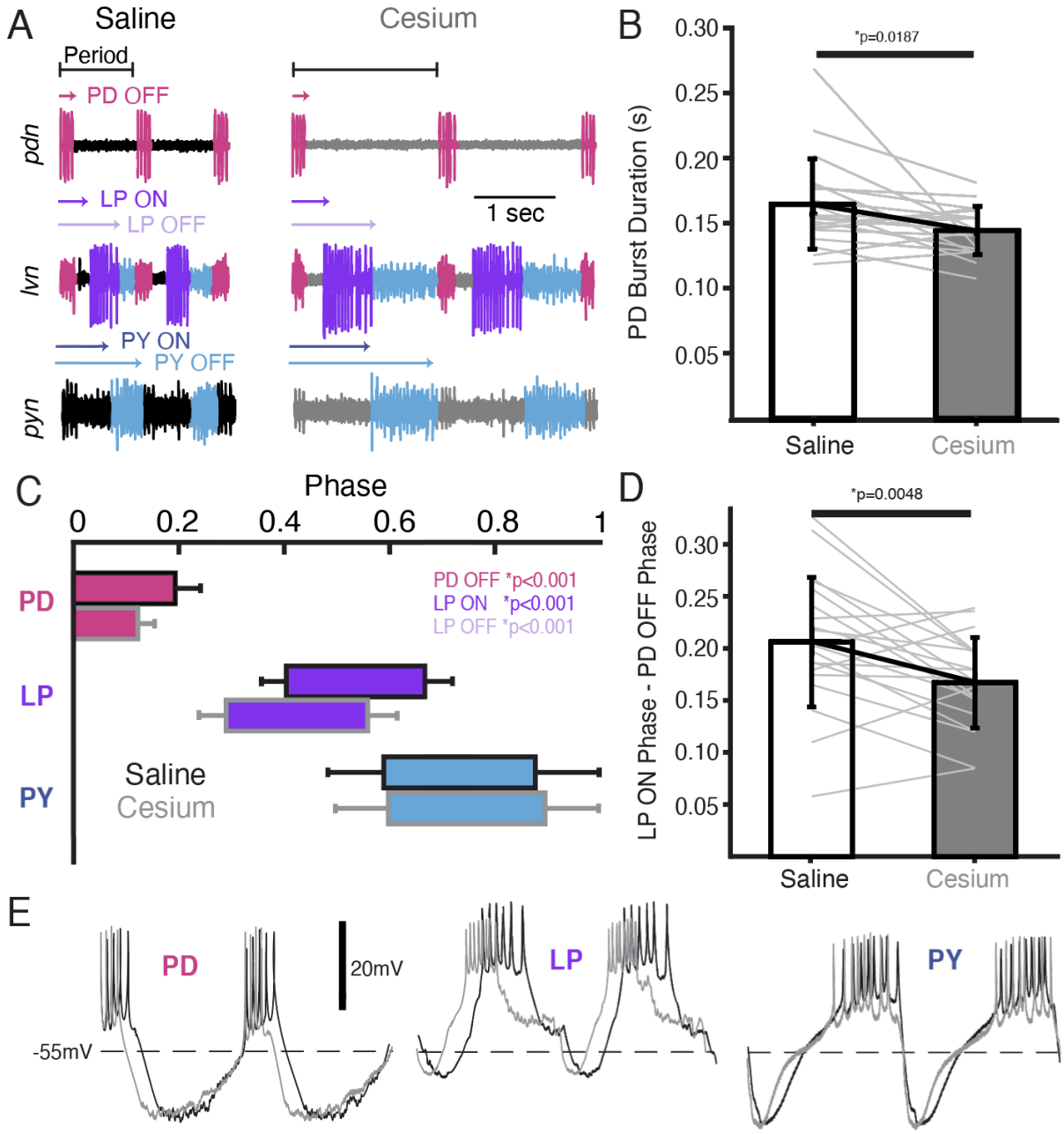

Figure 5: In Cs^+, PD OFF, LP ON, and LP OFF were all advanced compared to saline. **(A)** extracellular example traces of two pyloric cycles at 11°C recorded simultaneously on the *pdn* (**top**), *lvn* (**middle**), and *pyn* (**bottom**) in saline **(left)** and from the same experiment in Cs^+ (**right**). PD spikes are colored magenta, LP purple, and PY blue. Onset and offset delay of each neuron relative to the beginning of the period (PD burst) are indicated by arrows. **(B)** Duration of PD burst was marginally but significantly shorter in Cs^+ than saline (Wilcoxon Signed Rank Test, N=21, p=0.019). **(C)** Phase plot of saline and Cs^+ colored as in **A**. PD OFF, LP ON, and LP OFF are all advanced in Cs^+ compared to saline. **(D)** The phase delay between LP ON and PD OFF is smaller in Cs^+ than in saline (paired Student's t-test, N=21, p=0.0048). As such, LP ON is more

advanced than one would expect if the system was maintaining a constant phase delay between PD OFF and LP ON. **(E)** Two periods of example intracellular recordings from PD (**left**), LP (**middle**), and PY (**right**) in saline (black) and Cs^+ (grey) scaled to the same period. Each column is from a different experiment. Note the advance of PD OFF, LP ON, and LP OFF with relatively little other change in the overall trajectory of the voltage trace.

Phase	Saline	Cs^+	Significance Test	N	p-value
PD OFF	**0.19±0.04**	**0.12±0.03**	**T**	**21**	**<0.001***
LP ON	**0.40±0.05**	**0.29±0.05**	**T**	**21**	**<0.001***
LP OFF	**0.66±0.05**	**0.56±0.06**	**T**	**21**	**<0.001***
PY ON	0.58±0.11	0.60±0.11	T	12	0.86
PY OFF	0.87±0.20	0.90±0.19	W	12	0.91

Table 1: Mean phase of pyloric neurons in saline and Cs^+ at 11°C. Phases that were significantly different in the two conditions are bolded. T=paired Student's t-test, W=Wilcoxon Signed Rank Test.

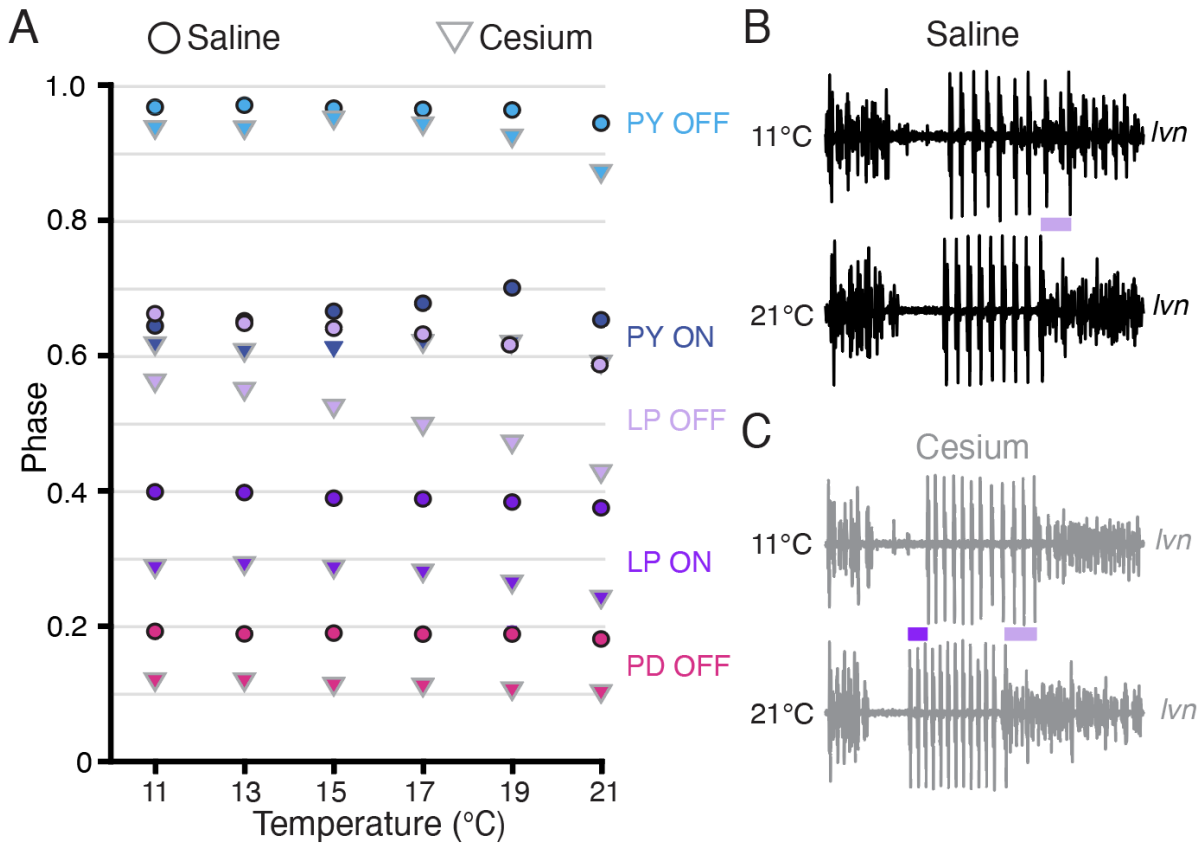

Figure 6: Phase advanced across temperatures for LP OFF in both condition; LP ON phase also advanced with increased temperature in Cs^+. **(A)** Mean phase as a function of temperature in both saline (circles) and Cs^+ (triangles) (N=21 for PD and LP, N=12 for PY). Error bars have been omitted for clarity. LP OFF advanced as temperature increased in both saline and Cs^+, though the advance in Cs^+ was more dramatic. LP ON also significantly advanced with temperature in Cs^+. Criteria for maintaining constancy was a mean slope of phase vs temperature across experiments that was significantly different from zero according to a Wilcoxon Signed Rank Test (if not-normally distributed) or a paired Student's t-test (if normally distributed), Bonferoni-adjusted. **(B)** Single period of pyloric rhythm recorded extracellularly on the *lvn* at 11°C (**top**) and 21°C (**bottom**) scaled to the same period. The advance in LP OFF is highlighted by the lilac bar. **(C)** Same preparation as in **B** but while in Cs^+. Lilac bar highlights the LP OFF phase advance, purple bar highlights LP ON advance.

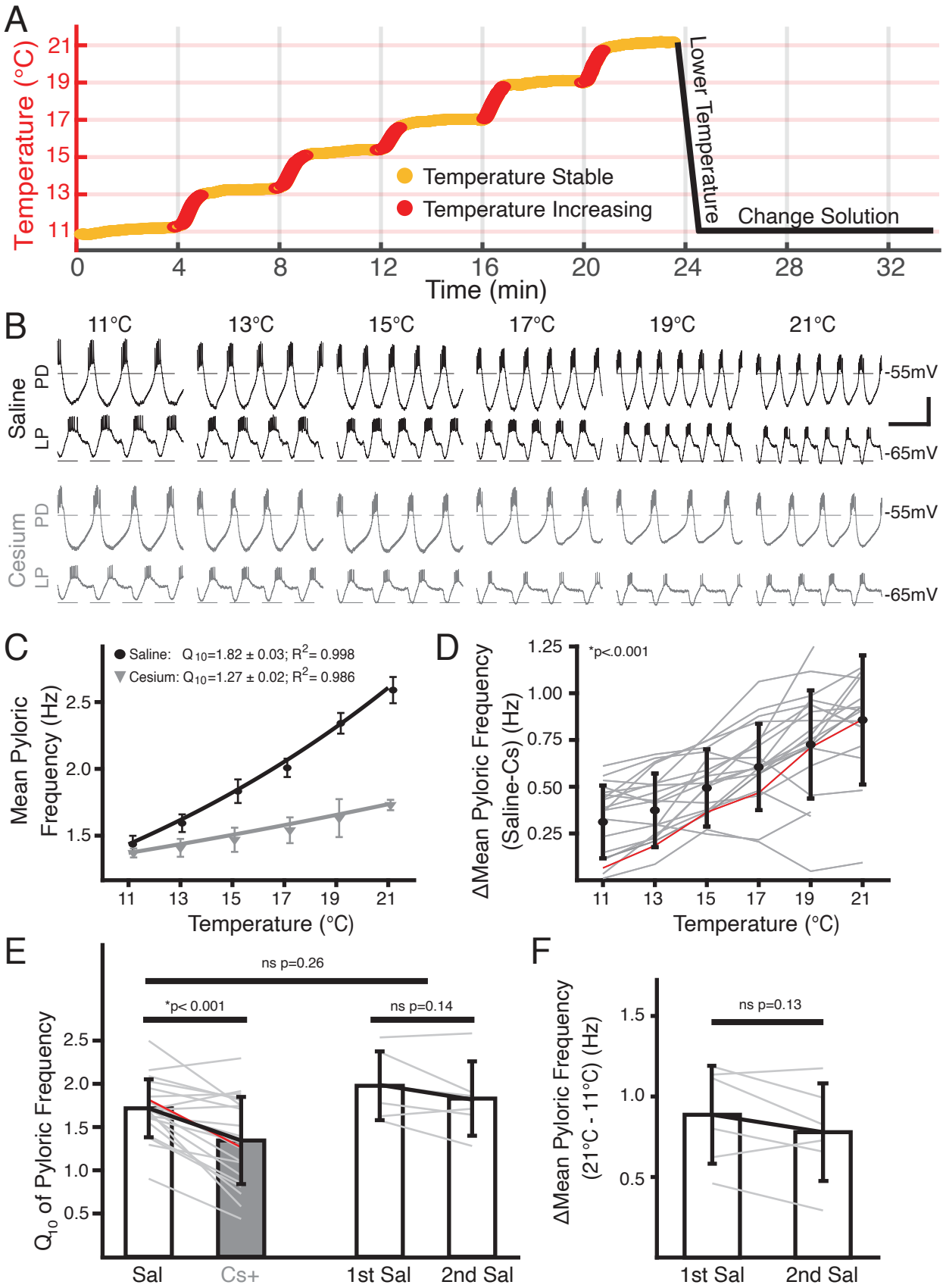
A
Temperature (°C)
21
19
17
15
13
11
Temperature Stable
Temperature Increasing
Lower Temperature
Change Solution
0
4
8
12
16
20
24
28
32
Time (min)
B
11°C
13°C
15°C
17°C
19°C
21°C
Saline
PD
LP
-55mV
-65mV
Cesium
PD
LP
-55mV
-65mV
C
Saline: Q10=1.82 ± 0.03; R2= 0.998
Cesium: Q10=1.27 ± 0.02; R2= 0.986
Mean Pyloric Frequency (Hz)
2.5
2.0
1.5
11
13
15
17
19
21
Temperature (°C)
D
*p<.0.001
ΔMean Pyloric Frequency (Saline-Cs) (Hz)
1.25
1.00
0.75
0.50
0.25
11
13
15
17
19
21
Temperature (°C)
E
ns p=0.26
*p< 0.001
ns p=0.14
Q10 of Pyloric Frequency
2.5
2.0
1.5
1.0
0.5
Sal
Cs+
1st Sal
2nd Sal
F
ns p=0.13
ΔMean Pyloric Frequency (21°C - 11°C) (Hz)
1.5
1.0
0.5
1st Sal
2nd Sal

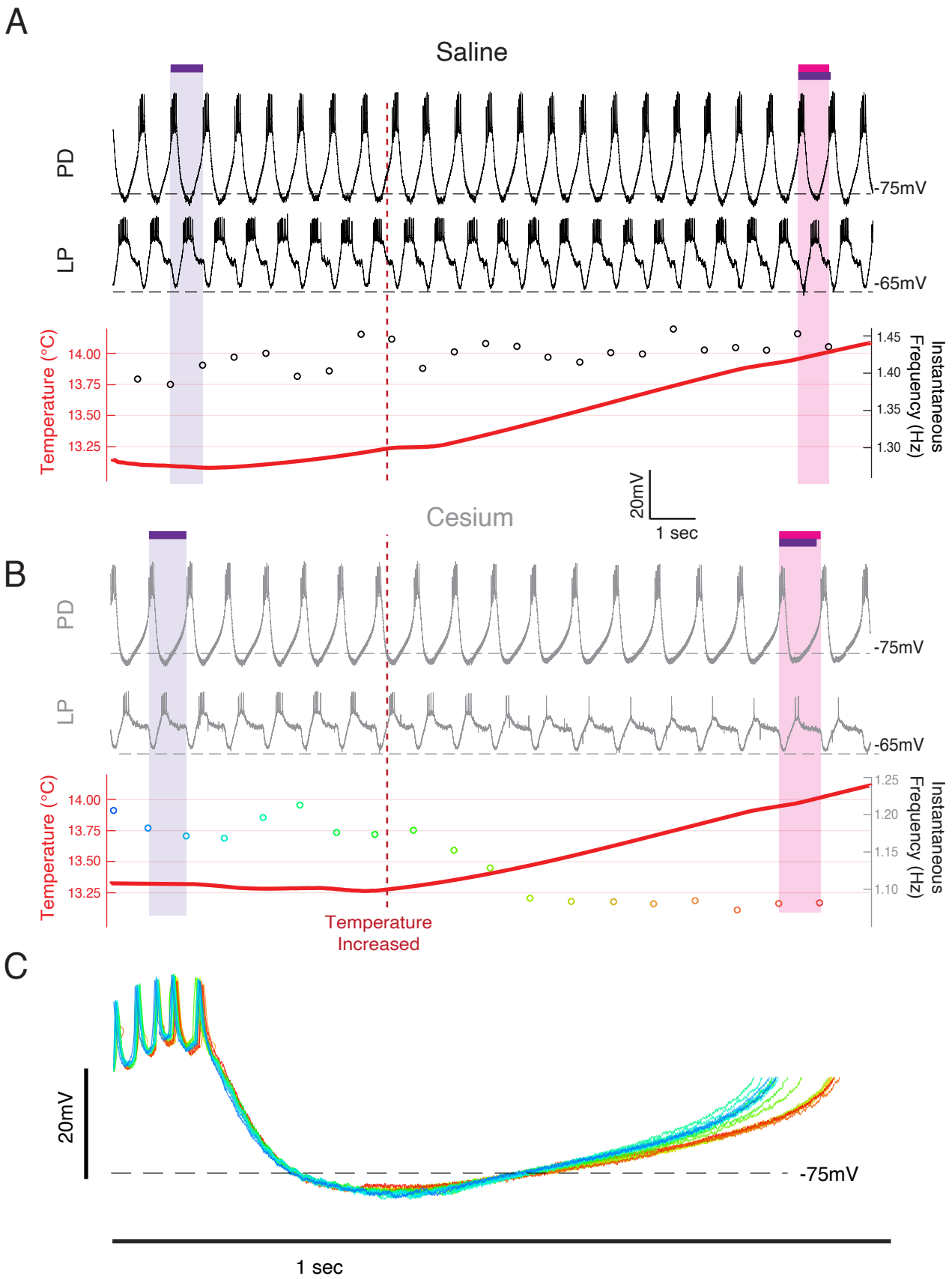
A
Saline
PD
LP
-75mV
-65mV
Temperature (°C)
14.00
13.75
13.50
13.25
1.45
1.40
1.35
1.30
Instantaneous Frequency (Hz)
20mV
1 sec
Cesium
B
PD
LP
-75mV
-65mV
Temperature (°C)
14.00
13.75
13.50
13.25
1.25
1.20
1.15
1.10
Instantaneous Frequency (Hz)
Temperature Increased
C
20mV
-75mV
1 sec

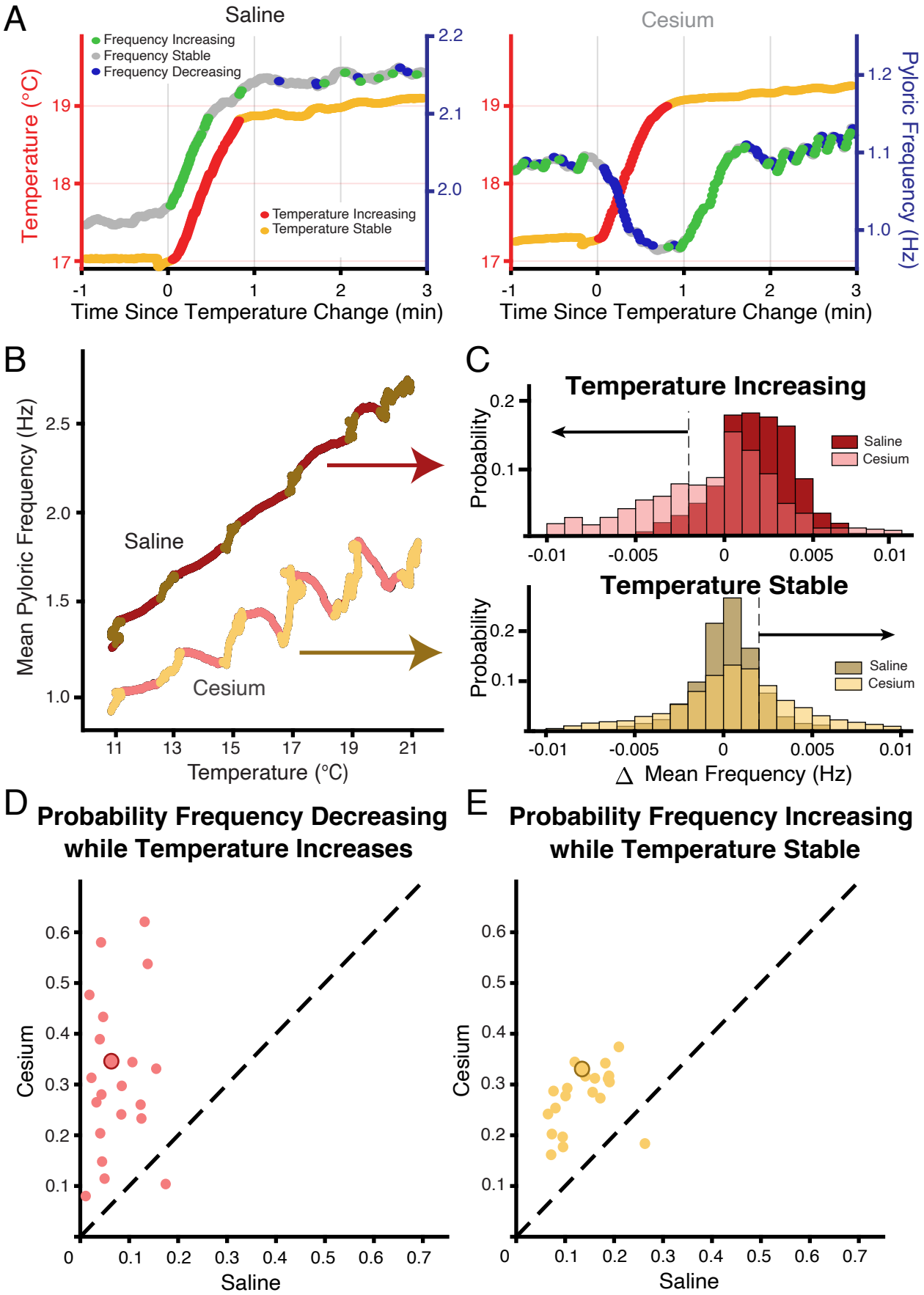
A
Saline
Cesium
Frequency Increasing
Frequency Stable
Frequency Decreasing
Temperature Increasing
Temperature Stable
Temperature (°C)
Pyloric Frequency (Hz)
Time Since Temperature Change (min)
B
Mean Pyloric Frequency (Hz)
Saline
Cesium
Temperature (°C)
C
Temperature Increasing
Temperature Stable
Probability
Saline
Cesium
Δ Mean Frequency (Hz)
D
Probability Frequency Decreasing while Temperature Increases
Cesium
Saline
E
Probability Frequency Increasing while Temperature Stable
Cesium
Saline

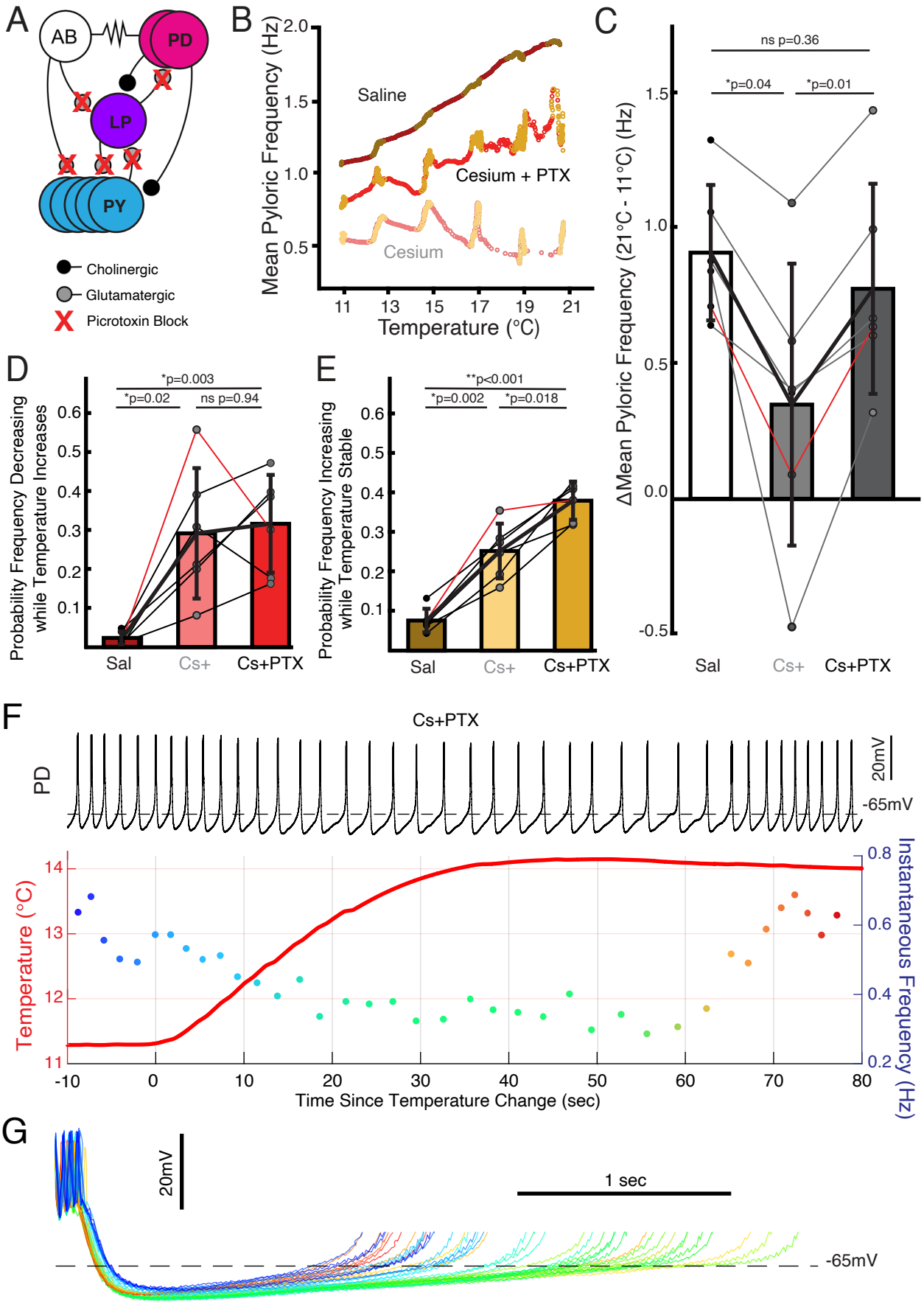
A
AB
PD
LP
PY
Cholinergic
Glutamatergic
Picrotoxin Block
B
Mean Pyloric Frequency (Hz)
Saline
Cesium + PTX
Cesium
Temperature (°C)
C
ns p=0.36
*p=0.04
*p=0.01
ΔMean Pyloric Frequency (21°C - 11°C) (Hz)
Sal
Cs+
Cs+PTX
D
*p=0.003
*p=0.02
ns p=0.94
Probability Frequency Decreasing while Temperature Increases
E
**p<0.001
*p=0.002
*p=0.018
Probability Frequency Increasing while Temperature Stable
F
Cs+PTX
PD
20mV
-65mV
Temperature (°C)
Instantaneous Frequency (Hz)
Time Since Temperature Change (sec)
G
20mV
1 sec
-65mV

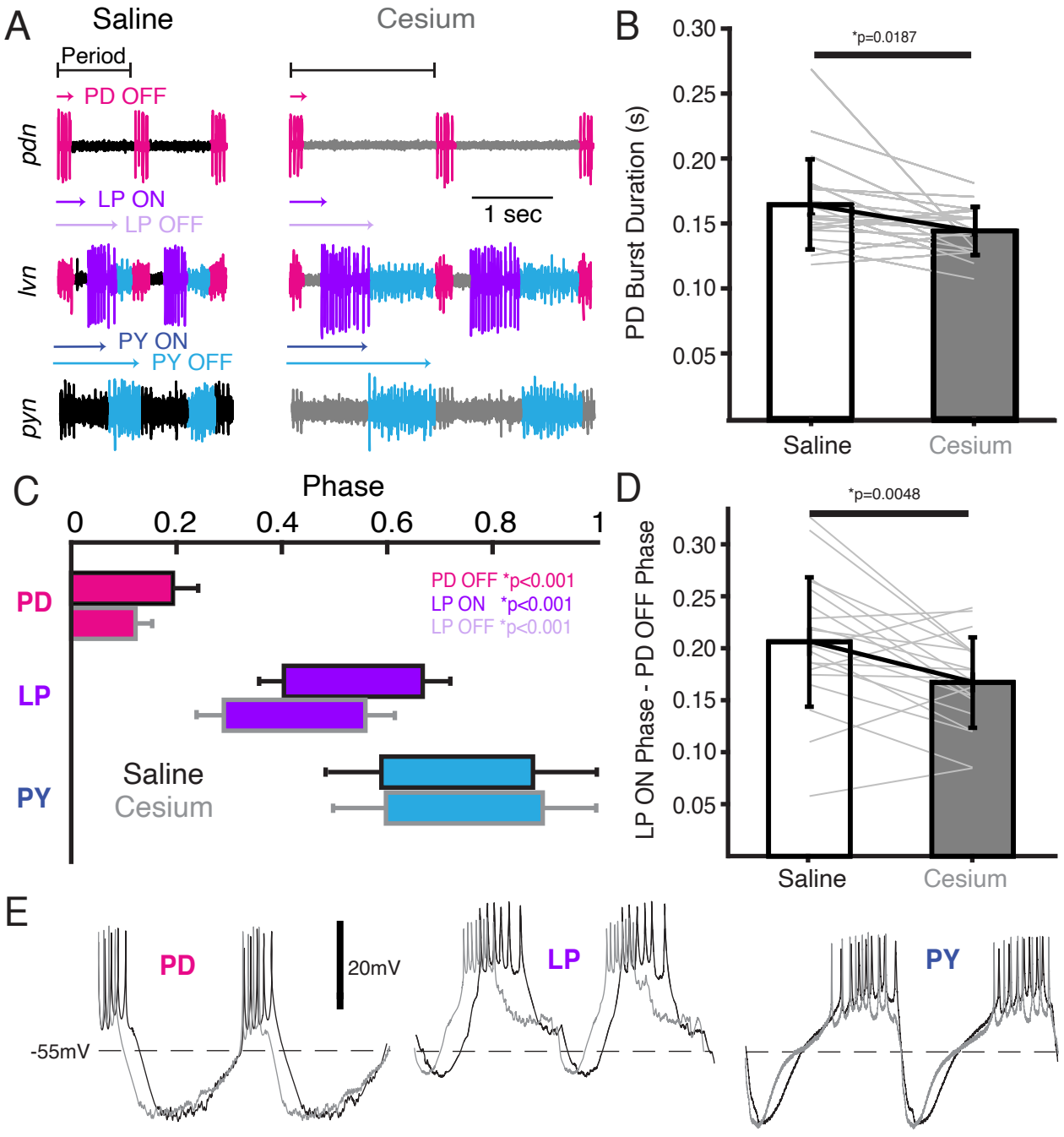
A
Saline
Cesium
Period
PD OFF
pdn
LP ON
LP OFF
1 sec
lvn
PY ON
PY OFF
pyn
B
*p=0.0187
PD Burst Duration (s)
0.30
0.25
0.20
0.15
0.10
0.05
Saline
Cesium
C
Phase
0
0.2
0.4
0.6
0.8
1
PD
LP
PY
PD OFF *p<0.001
LP ON *p<0.001
LP OFF *p<0.001
Saline
Cesium
D
*p=0.0048
LP ON Phase - PD OFF Phase
0.30
0.25
0.20
0.15
0.10
0.05
Saline
Cesium
E
PD
20mV
LP
PY
-55mV

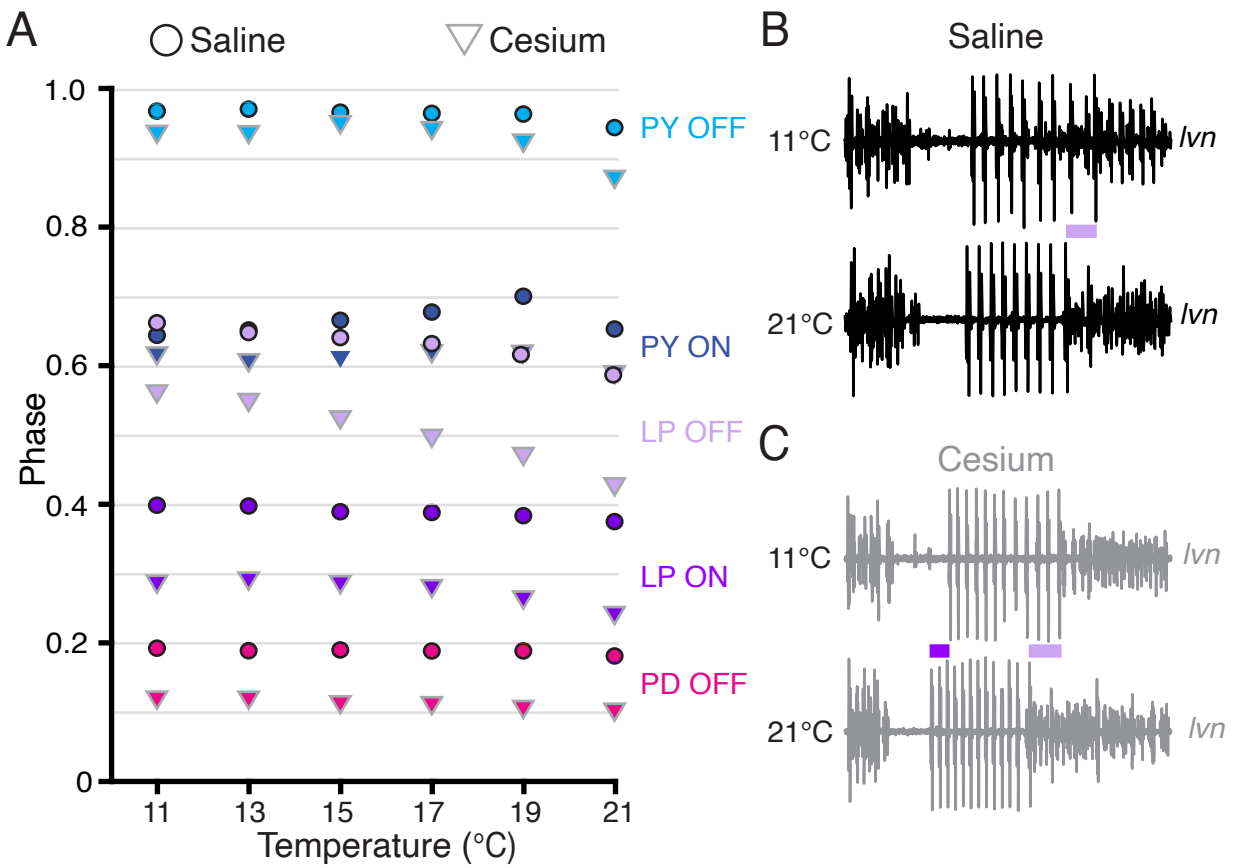
A
Saline
Cesium
1.0
0.8
0.6
0.4
0.2
0
Phase
11
13
15
17
19
21
Temperature (°C)
PY OFF
PY ON
LP OFF
LP ON
PD OFF
B
Saline
11°C
lvn
21°C
lvn
C
Cesium
11°C
lvn
21°C
lvn